Reviewer 1

Major comments

OBS1. Title I found the title misleading since the firn cores temporal extent is too short as to infer climatic signals from them. A suggested title would be: Water stable isotope and deuterium excess records from precipitation and firn cores from northern Antarctic Peninsula as tools for climate studies in the region.

ANS.1. The reviewer has a valid point here, as the word "climatic" could mislead the readers. Instead we propose the following title:

New regional insights into the stable water isotope signal at the northern Antarctic Peninsula as tools for climate studies

OBS2. Database I am concerned about the author's use of the Tair and altitudinal T profiles from BE station. Why the authors would expect this temperature to be representative for the core sites? Later in section 2.3 the authors mention that daily mean temperatures are available at OH, then why not to use that data set instead of the BE-data? Please elaborate and justify the use of the BE data set.

ANS.2. The BE dataset was used instead of OH, since the latest has numerous gaps of validated data (see: https://legacy.bas.ac.uk/met/READER/surface/O_Higgins.All.temperature.html). This is especially important for the most recent years. Some years (e.g.: 2015) even with 50% of the monthly data validated under 80% of daily temperature records. On the other hand, BE has an uninterrupted validated record from 1968 to the present. Both data sets (OH-BE) correlate (for validated months) with a *r*-value higher than 97% ($p<0.01$). This correlation is even higher than the correlation between the OH Station data and Esperanza (ESP) Station (96%), which is located less than 100 km away. However, ESP is located at the east coast of the Antarctic Peninsula and therefore, is partially influenced by continental conditions. The figure attached to this comment shows the linear regression and correlation for the OH-BE and OH-ESP datasets.

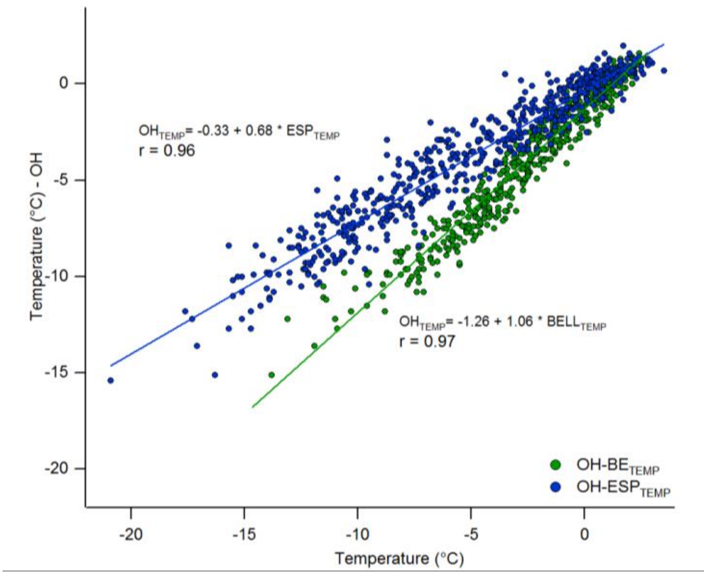

OBS3. Stable isotope time series analysis In section 2.3, page 5-25, the authors state that the d-excess signal obtained from the firn cores was depicted against depth and filtered using IFFT to be compared with d-excessmeteo, but the authors never showed the original raw core isotope data, nor discussed the quality of it, e.g. amplitude of the signal, seasonality, possible melt, signal differences /similitude at the different core sites, etc. The authors must describe the raw isotope data before applying any further statistical method to compare it with either instrumental or modelled data. Before assessing the quality and representativeness of the raw data it is not possible to carry on with other comparisons. Further, the authors obtained the time scale of core d-excess based on the "the strong similarities between both signals (d-excess and d-excess meteo)"; even thought this method is quite interesting and innovative, and both profiles clearly agree (Fig. 3), the authors must indicate why a more traditional dating was not preformed, e.g., annual layer counting, which would be the obvious first attempt on dating the cores. The authors must address this issue and justify the dating method used in order to show its value over more traditional approaches. The authors must also indicate the error in the time scale obtained. This is shortly introduced in the text in section 4.2 but it should be mentioned already in section 2.3.

ANS.3. The reviewer is right by addressing this comment, we certainly did not discuss properly the quality either the representativeness of the RAW data. We will add a new paragraph at the beginning of section 2.3, which will include a general description of the RAW data, a discussion about the quality and representativeness and we will also refer to the issues that we had attempting to carry out a traditional dating method. Furthermore, as it is suggested, we will highlight the value of the new method proposed over other more traditional approaches.

In relation to the displaying the RAW data, this is available from the assets to this publication:

https://doi.pangaea.de/10.1594/PANGAEA.871083

https://doi.pangaea.de/10.1594/PANGAEA.871080

Figure 3 already includes this data, nevertheless, the color that we have chosen was probably not the best one. We will change the color in this figure in order to represent the RAW data in a better way.

Since our dating was carried out using a signal-tuning method, the error associated with this method is usually dependent on the error that the reference signal has and also to the differences between the two signals that are compared. In our context, as both signals should be dependent on almost the same variables which have seasonal behaviors, the error associated with the signal matching can be estimated as to be of +/- 1 month.

OBS.4. Seasonality The authors define seasons and sample sets to each season. However, the authors have a limited number of years (2008-2014) as to construct a representative seasonal signal of d18O in precipitation at the study site to use as a baseline to compare with particular monthly means of a given year. The authors use 1 month of a particular year to describe a seasonal signal without discussing its representativeness. Therefore, the results must be explained as results for a particular year rather than as to a "seasonality", mentioning the results limitations.

ANS.4. This comment is right in relation to the seasonal long-term approach that we are not able to achieve with our limited dataset.
A paragraph will be added in section 4.1 specifying the limitations and representativeness of our dataset. We will highlight the fact that the information presented in this study is intending to give a rough idea about changes identified in the isotopic signal throughout the year in a short time span, rather than creating a regional baseline.

OBS.5. Glaciological setting The authors must provide a more detailed description of the study site, e.g. glaciological setting, meteorology of the study site, earlier studies of in the OH area, if available. This could be included in an additional section as "study site".

ANS.5.The authors believe that a new section is not absolutely needed. The introduction already describes most available (rather scarce) glaciological information for the study region. Others like meteorological and geographical references are widely discussed along this manuscript and in a previous work of this group (Fernandoy et al., 2012), also published in the journal. Nonetheless, we will add more details to the last part of the introduction section.

Minor comments

1-23. Be more specific when given the results. The results presented here are a snapshot of a region situated at Antarctic Peninsula but they don't necessarily reflect the whole Antarctic Peninsula situation. Unless a geographical significance study is done, please clearly state to which region of the Antarctic Peninsula are your results representative.

Ans*1-23*. This was corrected along the whole manuscript to emphasize that our discussion is valid for the most northern portion of the Antarctic Peninsula, i.e.: Study region close to the Laclavere Plateau and nearby west flank.

2-2. I have seen Antarctic Peninsula being referred as AP or APIS (when talking about Antarctic Peninsula Ice sheet), I wonder why the authors chose API.

ANS.2-2. The abbreviation API was taken for simplification reason from the sample codes analyzed here and used also on our previous publication. In order to keep a consistency with other authors from the region, we changed the abbreviation API to AP for this manuscript.

2-24. at several stations

ANS.2-24. Corrected as suggested

2-27. with a marked warming

ANS.2-27. Corrected as suggested

3-22. ***the authors only mention the "high temporal resolution" of their records but did not talk about the temporal extent of their records. Since the title of the manuscript involves climate, the temporal extent of the firn cores is as important as the resolution and should be introduced together.***

ANS.3-22. Corrected as suggested

4-3. ***austral summer campaigns***

ANS.4-3. Corrected as suggested

4-3: please remove "several shallow–depth firn cores (totalling more than 60 m) were retrieved from the northern part of the API". There is no need to add this vague information if the authors are going to give more details of the cores in the next sentences.

ANS.4-3. Corrected as suggested

4-4: Add link to Figure 1. Label O'Higgins station as "OH", also add info on image source and contours details.

ANS.4-4. Corrected as suggested

4-8: Please be more specific about how many samples were discarded and why.

ANS.4-8. Additional information was added to this section. The samples were discarded using a statistical outlier test (modified Thompson tau technique) (Thompson, 1985). Using this criterion all samples with d-excess values lower than -9‰ were discarded, as they lie outside the normal distribution of regular samples.

4-10/13. ...profile of density and physical properties of the ice

ANS.4-10/13. Corrected as suggested

10-13: add info of the drill, handling, storage, and sampling for all cores. This can be summarized in a table.

ANS.4-10/13. This information is included in section 2.1, however additional antecedents on the handling of water samples will be included in the manuscript.

4-16. ***To which institution/facility in Viña del Mar? Please add information about sample melting and storage during melting (type of vial). As mentioned by the authors in page 20-21, secondary processes during storage and transport (and also melting of the sample) can perturb the isotopic signal.***

ANS.4-16. As for the previous observation additional information of the protocol followed both in Chile and Germany will be included in section 2.1. This basically consist in melting the snow and firn samples at controlled conditions (4°C) in sealed bags overnight. At the next morning previous to running the isotope analysis, each sample was agitated for homogenization.

4-18. ***Indicate where the water stable isotopes were analysed (instrument, method, etc) and the accuracy for all the cores. This is depicted in Table 1 but it is not clearly stated in the text. Cite references to values shown in Table 1.***

ANS.4-18. As before, additional information was added and table 1 referenced as suggested.

4-18. ***Please indicate where the firn and precipitation samples were collected at OH.***

ANS.4-18. This information was added to 4-7

OBS. ***In Fig. 2, show source of the data. Please add the BE station in Figure 1.***

ANS. The source of the data (LIMA-Landsat Image Mosaic of Antarctica) was added to the figure. Station BE (Bellingshausen) is located on the South Shetland Island, therefore out of the scope of this image. An insert to this figure will be added.

5-1: ***Please indicate the arrival point of the HYSPLIT trajectories. Was 1-backtrajectory estimated or a cluster of backtrajectories?***

ANS.5-1. This information was added, corresponding to OH coodinates at an isobaric arrival point of 850 hPa (around 1500 m a.s.l.). The backward trajectory analysis corresponds to a cluster analysis and not single trajectories.

5-22. ***"for the whole region". The author's refer to the whole Antarctic Peninsula? If, yes, the authors might reconsider limit the interpretation to the nearby study area. It is unclear to me if the HYSPLIT backtrajectories were set to end at OH or to other sites in the Peninsula. Please clarify this.***

ANS.5-22. This was corrected to express that our discussion correspond to the nearby region of the OH Station and Laclavere Plateau, and doesn´t mean to extend this conclusions to the whole Antarctic Peninsula region, which clearly exceed the scope of this work.

Figure 3: ***it is not clear to me if cores OH-10, OH-9, and OH-6 were drilled at the exact point, how close were there drilled? This info cannot be inferred from Table 1 which shows the exact coordinates for all three cores. The core sites could be shown as a zoomed-in section in Fig. 1.***

ANS. The location was intentionally selected at the same position for the cores OH-6, OH-9 and OH-10, but retrieved in different years. This will be explained on the revised version of this manuscript.

6-25,26: ***this should be stated earlier in the text, e.g. in section 2.3 when figure 3 was shown.***

ANS.6-25,26. This paragraph was moved as suggested.

6-27: ***Remove OH***

ANS.6-27. Removed as suggested.

6-28: ***Please mention how many samples were rejected and why. This is mentioned earlier in the text but is not discussed.***

ANS.6-28. This information was added to section 2.1. A total of 13 precipitation samples were discarded.

Figure 6: ***please add labels for the study site, and Bellingshausen Sea in the map*****.**

ANS. Labels were added to the figure

7-6: ***please mention how the authors defined the seasons, e.g. DJF-! summer. Also, please explain better how you selected the set of samples representative of each season; as it is written in the text, it appears that the set for each season was selected upon the number of samples of arbitrary months which might cause bias, especially in section 3.1.1 where the seasonal regression slopes are discussed. Please consider using all samples available for each season or limit your discussion to the represented months but not to seasonal scales. Please discuss the annual precipitation distribution***
at the study site if available and put your results in that context. Also discuss how precipitation samples were taken, is a precipitation event identified as one precipitation sample or are the samples taken and identified on a daily (hourly) basis? Indicate in a figure the number of samples per month and also the volume per sample/event.

ANS.7-6. Done as suggested. Regarding the sample selection, we extended the explanation of our selection criteria. Related to precipitation sample acquisition, there was already an explanation in the text referring to the daily scheme in which precipitations were measured. Figure 7 shows the precipitation sample distribution.

7-9: ***Please discuss how outliers were removed in section 3.1.1 (when first referred).***

ANS.7-9. Done as suggested

7-11: ***please include the error and significance of the regression slopes.***

ANS.7-11. Done as suggested

7-13: ***the authors must justify why they believe a particular month is representative of a season. If the authors have data for all months, why to assume only one month as representative of a season? This issue has been addressed in a previous comment (7-6). This is very important to clarify as the authors are attempting to link their results to climatic features.***

ANS. 7-13. Answered in 7-6

7-16: An inverse behaviour between July and June or between July-June compared to MAM and SON? Please explain.

ANS.7-16. An specification was added to the text

7-22: do not use "weak", use instead: correlation coefficients for these comparisons are not significant (indicate level of confidence).

ANS.7-22. Done as suggested. Also the value of the rejected samples was wrongly stated in this section ("lower -2‰"), as showed before, the statistical outlier test points out to eliminate all samples deviating more than 2σ from the mean value (i.e.: <-9‰ and >12‰).

7:3.1.3 ***Please indicate geographical sites in a figure (in Fig. 6 for example).***

ANS. Done as suggested

Figure 8 ***can be removed and the equation of the regression line can be given in section 3.1.3.***

ANS. Figure 8. The authors consider that this figure is needed to give a better idea of the correlation for different values of d-excess. However, we do recognize that this figure is not key for the paper. We would still propose to keep this figure.

8-5: ***define GMWL and LMWL in the text (now is only defined in Fig. 9)***

ANS. 8-5. This was done as suggested.

8-6: ***previously you defined the slope as "s", now it is mean slope as "m" but not defined, either use s again or define mean slope as "m".***

ANS. 8-5. This was corrected throughout the paper to keep consistency using the "s" for slope.

8-9: ***Please remove the first sentence as it is unnecessary.***

ANS. 8-9. We considered that this sentence works as a short introduction for the following section. We think it should be kept in this sense.

8-10: ***as mentioned in a previous comment, a discussion about the quality of the isotope raw data must be addressed earlier in the text.***

ANS 8-10. We recognized this point and added a discussion on section 2.3

8-26: ***how the authors could explain the melt layers then if there is no signal of infiltration or connection with summer melt? Could the authors include the percentage of melt per m w.e.?***

ANS. 8-26. This issue will be discussed at the end of section 4.1

8-31: ***higher than the annual, monthly mean?, please specify.***

ANS.8-31. We mean monthly means, this was corrected in this section.

9-5: ***"monthly d18O-T relationship was considered to reflect seasonal behaviour" based on? Please add a discussion to explain the authors' assumption.***

ANS. 9-5. This phrase was eliminated from the text, as it was unnecessary and could lead to confusion of the following text.

5-9: ***what is the general trend? The data sets are too short as to describe or assume they represent a general trend.***

ANS. 9-5. This was revised and corrected in the text

9-15: ***please indicate the basis to the -1.4C latitudinal correction. Also indicate lapse rates used.***

ANS. 9-15. The correction procedure was now added to this section, the basis of doing so is previously exposed on the major comment 2.

9-16: ***Indicate the significance of the trend, this is important due to the short period covered (only 5 years).***

ANS. 9.16. This information was added to the revised version of the text

Figure 10: ***indicate the resolution of the temp. data.***

ANS. Added to the figure "monthly resolution"

9-20: ***indicate significance of the trend.***

ANS. 9-20. Done as suggested

9-25: ***of which station? Please specify.***

ANS. 9-20. OH (BE) station was added to this sentence.

10-30: ***replace "clear" with significant or not significant.***

ANS.10-30. This sentence was modified, as it doesn´t mean to point out an statistical trend, but rather a tendency of increase in density of the firn pack.

10-3.2.3 Is there any evidence of wind redistribution of snow that could be operating at lower elevations? How is the amplitude of the seasonal d18O cycles at different elevations? Is there any sign of melt at lower elevations?

ANS. 10-3.2.3. This matter was not discussed here in extent, since was already exposed by Fernandoy et al. (2012). A noticeable effect of melting is present bellow 700 m a.s.l., that it´s location of OH-4 and bellow. Wind redistribution will play a role in some geographical singularities like depression or valley-like features. All cores were retrieved from geographical height in order to minimize this effect (Fernandoy et al., 2012). Nonetheless, these redistribution effects are much less important against the high accumulation rates for this region.

11-27: compositions

ANS. 11-27. Corrected in the text.

11-14: ***I would be cautious to extrapolate the results to the whole Peninsula region and rather specify that the result is valid for the study site. Reference to data from additional sites at the Peninsula is needed as to assure what the authors claim. The authors also need to address that the time extent of the cores prevent to robustly interpret their results into a climatic scenario. The results presented in the study are a snapshot representing and must be carefully put into a climatic context in order to avoid speculative interpretations.***

ANS. 11.14. This observation was taken into account along with other previous similar observation referring the regional vs. local extension of our results. We will revise the text to make it clear, that our investigation shows the situation for a specific portion of the Antarctic Peninsula (i.e.: northern AP) and for a restricted time frame (2008-2015).

11-18-20: ***The authors need to show evidence of similar findings elsewhere in the Peninsula as to support their claim, otherwise the claim is highly speculative when extrapolating the study results to the whole Peninsula area.***

ANS. 11-18-20. We will restrict our discussion concretely to our study region, since similar study are non-existent or scarce to rest of the Peninsula.

Figure 12: ***please correct x-axis label to "sea ice extent". Indicate the SIE data source. Indicate also the definition of the SIE index used.***

ANS. 12. The axis of figure was modified accordingly, and the source and definition of SIE was added. SIE data was obtained from the NSIDC Sea ice index (https://nsidc.org/data/seaice_index/) and the definition of the sea ice extent is according to . Defining the edge of the sea ice, as the portion of sea surface covered by at least 15% of ice.

12-8: ***it is important to address if the trend is significant or not.***

ANS. 12-8. As in previous observation, we don´t mean to express a statistical trend of the isotope values, but rather a tendency of depleted values with higher altitudes. This will be corrected on the text.

12-20: "ice layers likely developed by wind ablation on wind–scouring processes at the plateau." Could the authors explain how wind could create ice layers?

ANS. 12-20. In this line we expressed our self not right. We actually don´t mean to state that a proper ice layer could form purely from wind in a high accumulation region like the AP. We refer here to actual glazed (ice) "crust", only a few mm wide as shown by the stratigraphy of the firn cores. This wind crust could form a thin glazed surface due to sublimation and snow drift abrasion, and in some opportunities by solidification of super-cooled droplets flowing against ground surface irregularities (sastrugi-like). During our field work, we witness these processes during different years.

References

Fernandoy, F., Meyer, H., and Tonelli, M.: Stable water isotopes of precipitation and firn cores from the northern Antarctic Peninsula region as a proxy for climate reconstruction, The Cryosphere, 6, 313-330, doi: 10.5194/tc-6-313-2012, 2012.

Thompson, R.: A Note on Restricted Maximum Likelihood Estimation with an Alternative Outlier Model, Journal of the Royal Statistical Society. Series B (Methodological), 47, 53-55, 1985.

Reviewer 2

Major comments

OBS.1. There is a need to be more explicit about what datasets were used and exactly how. I would also like to see a better justification of their inclusion over perhaps more suitable datasets. This relates to observations (e.g., why use Bellingshausen station observations over the more proximal O'Higgins?) and the gridded datasets (why use HadISST versus a higher resolution observed SST dataset, and why not use the sea ice data from this same gridded dataset as opposed to using the NSIDC sea ice extent index). Also, how sea ice extent was measured is not explained in the manuscript.

ANS. We added to the manuscript an explanation, emphasizing which datasets were selected and how they were considered in this work. In relation to choosing Bellingshausen (BE) station over O'Higgins (OH) station, BE dataset was used instead of OH, since the latest has numerous gaps of validated data. (see: https://legacy.bas.ac.uk/met/READER/surface/O_Higgins.All.temperature.html). This is especially important for the most recent years. Some years (e.g.: 2015) even with 50% of the monthly data validated under 80% of daily temperature records. On the other hand, BE has an uninterrupted validated record from 1968 to the present. Both data sets (OH-BE) correlate (for validated months) with a *r*-value higher than 97% ($p<0.01$). This correlation is even higher than the correlation between the OH Station data and Esperanza (ESP) Station (96%), which is located less than 100 km away. However, ESP is located at the east coast of the Antarctic Peninsula and therefore, is partially influenced by continental conditions. The figure attached to this comment shows the linear regression and correlation for the OH-BE and OH-ESP datasets.

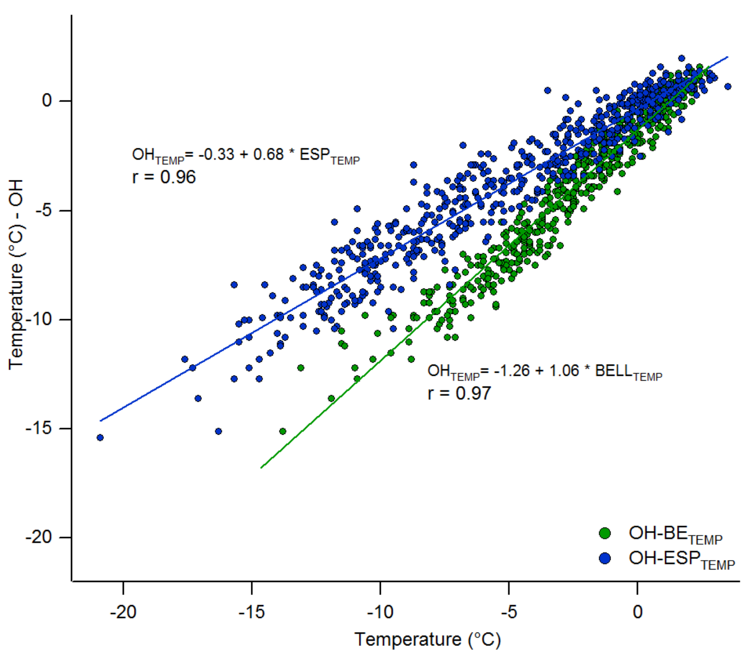

In relation to the gridded datasets, we have corrected the text since we unintentionally made a mistake writing HadISST, instead of HadSST. For Sea Ice extension we did not use HadISST since one of its key limitations is that higher resolution and more homogenous data are available for the modern satellite period, 1979-present. Instead of HadISST, we used NSIDC because it provides a higher resolution grid (25km x 25km). The reviewer is right by noticing that the way in which sea ice extension was not detailed in the text. To measure the sea ice extent we considered as a starting point the location of O'Higgins station and as an end point, the sea ice front in the direction towards King George Island. This procedure will be added to the manuscript.

OBS.2. To estimate dexcess meteo from the air parcel source region, SST seems to be from a fixed region whereas relative humidity was determined based on the HYSPLIT trajectories. Is this correct? And if so, why not just pull SST time series from the same geographic area as the RH reanalysis data? The regressions between observed temperature and isotopes as presented in sections 3.1.1 and 3.1.2 are not clear. Adding these regression scatter plots to Figure 7 would help.

ANS. The SST datasets were obtained from a fixed region based on two main reasons. The first one, because the continuity of the data in this quadrant during the time that we cover is more consistent than the neighbors, which in turn are rather limited and containing important gaps. The second reason is because almost all the air parcels that reached Laclavere Plateau, in the time interval studied, crossed through this region during a significant amount of time (one day or more). Thus, it might has likely exerted an imprint over the moisture parcel crossing this area. In contrast, out of this region, the pathways followed by the air parcels spread into different directions, characterized by data gaps and sometimes inconsistencies.

Even though the SST data considered is originated from a single region, considering a rough value of the behavior of SST at this latitude is enough to estimate dexcess meteo. As we show in the text, this parameter is less dependent of SST values (mostly influenced by humidity). Therefore, dexcess meteo is highly dependent of relative humidity. The 3-day backward trajectories provided data along the whole path, those data sets were considered to give representativeness to dexcess meteo estimation.

Linear regression were not added to the figure, but were discussed now in the text in section 3.1.1 and 3.2.2.

OBS.3. The regression between firn core derived dexcess and that derived from the gridded datasets (dexcess meteo) seems circular given that the gridded dataset-derived dexcess meteo was used to date the firn cores. There are multiple instances where the correlation between the core dexcess and the dexcess meteo is used to validate various parameters and interpretations of the core (including the dating), and I don't think this is supported because the firn cores were dated by peak matching with the dexcess meteo time series. If I am understanding this correctly, I believe the authors should revise the use of correlations between the two time series to support their analyses. I have documented some of these instances my comments below, but there are several other instances in the discussion that I have not mentioned.

ANS. The reviewer is right by addressing this comment, we committed an unintentional error in the caption of Figure 8. As it was written at the end of in section 3.1.3 "From the relationship between monthly mean values of d_{excess} from precipitation samples and $d_{excess\ meteo}$ constructed from meteorological parameters (*rh* and SST) of the high density precipitation pathways, a correlation coefficient of R= 0.86 ($p<0.01$) was obtained (Fig. 8)", the regression reflects the relation between dexcess from precipitations and dexcess meteo. The relation between both parameters is what we consider that validates the dating procedure, as precipitation dexcess is highly related with the constructed dexcess meteo. We will correct the figure´s caption accordingly.

OBS.4. The lack of melt in the cores is surprising given warm summers in this region and the literature cited in the introduction.

ANS.4. We haven´t neglected the effect of melting, however melt events are rather insignificant against the very high accumulation. During none of the field works (January – February) we have witnessed any major melt event at the highest point of the northern Antarctic Peninsula (i.e.: Laclavere Plateau). The stratigraphic profiles of the firn cores retrieved show different kind of ice layer/crust. We have attributed this to different phenomena like wind sublimation, precipitation of super-cooled humidity and in some cases possible melt layers. Nonetheless, we don´t see any possible seasonality in the distribution of the ice layer and crusts.

Specific comments:

Page 2

Line 4: Bromwich et al 2013 focuses on the central West Antarctic Ice Sheet air temperatures. I would suggest changing this reference to one that focuses specifically on Antarctic Peninsula air temperature trends.

ANS. Changed this citation to Carrasco (2013), and also indicated that this refers to the Antarctic Peninsula specifically.

Line 8: Change to "have recently lost mass"

ANS. Done as suggested

Line 9: Most modeling studies have shown that surface melt, though accelerated in places regionally, plays little direct role in the mass balance today. Only on the northernmost AP does it impact SMB, and only indirectly via ice shelf stability forcing, does it impact mass balance elsewhere – and today this is limited to the AP.

ANS. Added to the text that this refers mostly to AP

Line 12: Change "is losing" to lost

ANS. Done as suggested.

Line 13: Change "surpasses" to surpassed

ANS. Done as suggested

Line 14-15: Change to "This demonstrates how sensitive the coastal region of West Antarctica is to increased…"

ANS. Done as suggested

Line 16-17: I believe Trusel et al 2012 and Kuipers Munneke et al 2012 did not report significant positive trends in AP surface melt as whole. However, Abram et al 2013 and Trusel et al 2015 (Nature Geoscience) both note positive surface melt trends on the northeast Antarctic Peninsula from an ice core and from climate models and observations, respectively. I would suggest revising this sentence.

ANS. The lines were rephrased to clarify these points, as the reviewer make a valid point suggesting so.

Line 19: The first part of this sentence needs a citation indicating what studies show more wide-spread surface melt since the mid 20th century.

ANS. This was included and corrected according to the previous observation.

Line 31: Do the authors mean "tropical" ?

ANS. We refer to regular (pre-industrial period) patterns. We will include this information to this line.

Line 32-33: The "southern oscillation" is not another term for the SAM, but rather ENSO. Please revise.

ANS. This is correct. Southern Oscillation is misplaced; we will remove this term from cited line.

Page 3

Line 5: I would suggest citing Orr et al. 2008 (J. Climate) in reference to summer airflow over the AP owing to westerly wind increases.

ANS. Two cites were included to this line showing the impact of summer airflow: (Orr et al., 2008; van Lipzig et al., 2008)

Line 15: Please change to "hampers accurately determining"

ANS. Done as suggested

Line 16: Please change to "Therefore, climate models are necessary to extend the scarce climate data both spatially and temporally."

ANS. Done as suggested

Page 4

Line 8: Could you please expand upon what you mean by "improper storing"?

ANS. This was also brought up to our attention by referee 1 and clarified in the text

Line 28: Please indicate in the text how far Bellingshausen station is from the firn core sites and O'Higgins. Also, why were observations from O'Higgins not used?

ANS. Same as before. Referee 1 asked about this in his comments. We responded showing that OH data has long non-validated data periods. On the other hand, BE has an uninterrupted record since 1968. Although BE is located around 150 km NE from OH station, the correlation between both records (for valid period) is higher than 0.97 with a high statistical significance ($p<0.01$), which is higher than other station like Esperanza (ESP) ($r= 0.96$) located less than 100km from OH, but on the east side of the AP. Linear regressions show that OH and BE data has a slope very close to 1, while OH-ESP is lower ($s = 0.33$) (with lower r). This probably reflects some influence from continental conditions. Therefore, we used BE to complement the OH data. Figure attached here.

Line 31-32: HadISST is actually on a 1 grid. Did you use a different version of the data product? Also, why was HadISST chosen over a more strictly observational SST dataset (e.g., AVHRR, AMSR-E) or the 0.25 NOAA OISST v2 product? Given the cores only go back to 2008, I would think that using observations would be the best route. The use of HadISST (and the actual resolution used) should be further justified.

ANS. This was explained before. Please see answer to Major comment 1.

Page 5

Line 7: Did you use 1 day back trajectories or 3 day? If only 1 day as specified here, why on line 1 do you state 3 day? The methods here are a bit unclear. For example, did you calculate the RH only across the areas with >50pct parcel frequency (or some other threshold)? Also, could you reference Figure 6 here?

ANS. We first used 3 day backward trajectories to figure out the provenance and distribution of air parcels that reached the study site. As we noticed that there was a high density pathway in the region, we explored the conditions that prevail in the near surroundings (limited by 1 day backward trajectories). After analyzing both datasets, we determined that the area covered by 2 day backward trajectories had a high representativeness of the maritime region that surrounds Laclavere Plateau. This area is representative because geographically includes the region affected by westerly winds and sea ice front during winter time, both factors that exerts high influence on the air parcels that approach this region.

Line 14-16: It is unclear what sea ice metric was used to define sea ice extent "around the API". Was total Antarctic sea ice extent provided by the NSIDC Sea Ice Index used? If so, that dataset is certainly not suitable for the more regional/local analysis of this manuscript. This also raises the question of why not use the sea ice concentration data that are also part of the SST dataset (whether that is HadISST, if justified, or one of the higher resolution datasets)?

ANS. This information was now included in the text and we think it is better clarified now.

Line 18-20: This information is repetitive with the previous paragraph.

ANS. Modified in the text

Line 24: Please change "obtained" to "derived" or "estimated"

ANS. Done as suggested

Page 6

Line 6: Change "has been proved" to "has been proven" or similar. Section 2.4 more broadly: Was a constant wave velocity chosen to convert two way time to depth? Certainly the firn here is quite heterogeneous given high surface melt rates. Also, was the surface actively melting during the January fieldwork?

ANS. Proved was replaced. Regarding section 2.4: Radar results were revised and re-analyzed. We now used a 2D model velocity based on the density profile obtained from the local cores for the upper snowpack and a density model for deeper snow/firn. During January, we were in the field for about 10 days. We experienced days of strong snow precipitation, wind drift and also sunny days, but we didn't see evidences of surface melting in this short period.

Page 7

Line 6: Change "seasons"' to "season's"

ANS. Done as suggested

Line 10-11: Considering the "considerable differences" between daily and monthly mean isotopic values, could you please show standard deviation error bars on your monthly mean time series in figure 7?

ANS. Explained on major OBS. 2 this discussion was addressed in the text in section 3.1.1

Line 11-16: The regression analysis presented here is quite unclear. Is the regression slope derived from 3 points each for MAM and SON? Or, are you regressing daily values? Please consider revising the text here and adding a figure to show these regressions. This would be very helpful. Also, why are only fall and spring values being regressed (or were the other seasons regressed individually, but the results were insignificant?)? Please expand on this here.

ANS. The regression slopes presented were derived from d18O daily values from precipitation samples and mean air temperatures from those days. We will add a paragraph in the manuscript which will include the slope from other seasons and the standard error and significance of each slope. Additionally, Figure 7 will be modified to include an histogram to represent how precipitation samples are distributed in time, seasonal regressions will be discussed in the text in section 3.1.1. and 3.2.2.

Page 8

Line 2: This correlation testing seems circular to me. The d excess (meteo) was used to date the ice cores by aligning the ice core d excess vs depth profiles with the d excess (meteo) vs time. So, we should clearly expect a high degree of correlation to result since these time series are already manually aligned

ANS. As explained on comment 3 this is not what we intended. Please see explanation above.

Line 8: This paragraph seems better suited for the methods section.

ANS. We consider that this section should be kept here, it is through that some part of the methodology is revised here, but still showing results of combined geophysics and stable water isotope information.

Line 9: Please change to "allowed us to derive"

ANS. Done as suggested

Line 13: Again, the methods need to be more clear about the time frame analyzed using the back trajectories. Here it is stated 2 days, but elsewhere it says 3 days and 1 day.

ANS. The answer related to this subject is written in the comment of Page 5 Line 7

Page 9

Lines 1-3 / Figure 10: The stated relationships in the text are quite difficult to see on the plot. Could you plot this instead as a scatter plot, or perhaps highlight these areas on the existing line plot? Only January is labeled on the plot, with one other tick at July (?), so it's hard to understand. Please consider revising Figure 10 to improve clarity.

ANS. The figure was modified showing now the period of positive/inverse relationship and the time (x) axis better labeled.

Line 5-7: The methods used here for extending or contracting the relationship is unclear. Please revise.

ANS. This paragraph intends to refer to the fact that at this latitudes, calendar seasons do not play a significant role as climatic seasonality extends beyond calendar time limits. Rather than using calendar seasons we turned to define three seasons: winter (JJAS), summer (DJF) and a transitional season (MAM-ON). There paragraph will be corrected in the text in order to better address this issue.

Line 15: Methods for determining a latitude temperature correction unclear. Please clarify.

ANS. Done, new information is in the text now.

Line 16-17: Figure 12b does not show the mean annual air temperature or a negative trend over time. Please revise figure citation or consider adding this information in a figure.

ANS. Figure citation was revised as suggested.

Line 17-20: Methods for determining temperature using the meteorological observations and sea ice extent (how was this measured?) is unclear. Please revise and consider adding a figure showing these monthly correlations.

ANS. To clarify this observation, we redefined our equation to take into account the seasonal behavior in these region. We separated our equation in two branches which are dependent on the presence of sea ice. In moths with presence of sea ice in this region (May-June-July-August-September) the temperature was obtained by Tlcl= (Tbe-1.4) + 1,13(Mmonth*SIE+Nmonth), where Mmonth and Nmonth are the slope and interception of the linear relation between lapse rates and

SIE presented in Figure 12. On the other hand, during months without the presence of sea ice, the temperature over the Plateau was obtained by the expression Tlcl= (Tbe-1.4) + 1,13(H(x)), where H(x) is the monthly mean lapse rate value of a given month "x" measured in Bellingshausen Station between 1978-1996.

This paragraph will be corrected in the manuscript

Line 28: Please show the linear regression showing the -0.008 per mil slope on Figure 13a as opposed to the linked dots. Please also show for Figure 13b.

ANS. Figures were revised and changed as suggested.

Page 10

Line 6: Figure 14a only shows accumulation through 2014.

ANS. The most recent core analyzed goes to January 2015, therefore is not possible to have the accumulation for 2015. New cores from 2016 are yet to be analyzed will give more information about accumulation.

Page 11

Line 11-13: Again, these datasets were aligned, so the correlation reporting is circular.

ANS. As explained on comment 3, please see explanation. After taking into account our correction, the text makes sense since both parameters are independent.

Line 15-16: This could be interesting – where did the anomalous humidity air parcel originate according to the back trajectory analysis?

ANS. These trajectories are coming mostly form eastern coast of the Antarctic Peninsula and the continent, therefore reflecting depleted isotope values.

Page 12

Line 2: I would suggest revising the use of "natural" here when referring to SAM, given the anthropogenic forcing on SAM (ozone and GHG), which is appropriately acknowledged earlier in the manuscript.

ANS. To avoid confusion the word "natural" was eliminated and the phrase changed to "seasonal oscillations"

Line 17-19: I think this should be stated in reverse – that the isotopic composition is not altered by surface melt infiltration and percolation.

ANS. Corrected as suggested.

Line 20-21: I find the lack of ice layers in the firn cores due to surface melt refreezing to be unexpected. The mean monthly temperature at O'Higgins is often at or above 0°C during summer months. Do the lower elevation cores (300-600 m elevation) not have significant melt? And are smaller ice layers not present at the plateau cores? Even at -4-7°C mean monthly temperature (assumed using lapse rate for the 1100m plateau), I would expect melt each year. These layers

may not coincide with summer seasons based on your age-depth scales, which is common due to melt percolation into deeper layers.

ANS. Certainly lower areas show clear sign of melting, this was widely discussed on our previous work by Fernandoy et al. (2012). We identified that melting is strong even, for the high accumulation of this region, at altitudes lower than 700 m a.s.l. As addressed before, during all of our field season (all of them between January and February), we haven´t witnessed important melting events. Although we have seen the freezing of super-cooled droplets in the irregular surface (sastrugi-like) and glazed surface due to ablation by strong wind, accompanied by snow drift.

Page 13

Line 24: Should this say "altitude"?

ANS. We actually do mean latitude, referring to west flank from the AP divisory from Laclavere.

Page 15

Line 1: Should this say "manually"?

ANS. To avoid confusion we will delete the word mainly.

Line 8: Should this say between 2008 and 2014? I don't believe any data before 2008 are presented.

ANS. Typeset error. Thanks.

Line 9: Change to "proxies".

ANS. Done as suggested

Page 16

Line 3: I look forward to seeing longer records from this area!

ANS. We expect to continue the work in this area, further campaigns are planned for 2017/18.

Figures

Figure 1

It would be helpful to have an inset of the Antarcitc Peninsula (or perhaps even just the northern Antarctic Peninsula). In particular, having Bellingshausen station located on this map would be helpful given that some of the meteorological data analyzed are from this site. Also, a box showing the area where SST data were extracted would be helpful.

ANS. A second panel was added to this figure to show the location of both Station and LCL.

Figure 7

The small dots plotted differ from the legends and caption. Notably the "small orange dots" in (b) appear the same as the small dots in (a). Please revise this figure (also see comment from page 7 about adding error bars).

ANS. Revised. The figure was improved accordingly.

References

Carrasco, J. F.: Decadal Changes in the Near-Surface Air Temperature in the Western Side of the Antarctic Peninsula, Atmospheric and Climate Sciences, 03, 7, doi: 10.4236/acs.2013.33029, 2013.

Fernandoy, F., Meyer, H., and Tonelli, M.: Stable water isotopes of precipitation and firn cores from the northern Antarctic Peninsula region as a proxy for climate reconstruction, The Cryosphere, 6, 313-330, doi: 10.5194/tc-6-313-2012, 2012.

Orr, A., Marshall, G. J., Hunt, J. C. R., Sommeria, J., Wang, C.-G., van Lipzig, N. P. M., Cresswell, D., and King, J. C.: Characteristics of Summer Airflow over the Antarctic Peninsula in Response to Recent Strengthening of Westerly Circumpolar Winds, Journal of the Atmospheric Sciences, 65, 1396-1413, 10.1175/2007JAS2498.1, 2008.

Thompson, R.: A Note on Restricted Maximum Likelihood Estimation with an Alternative Outlier Model, Journal of the Royal Statistical Society. Series B (Methodological), 47, 53-55, 1985.

van Lipzig, N. P. M., Marshall, G. J., Orr, A., and King, J. C.: The Relationship between the Southern Hemisphere Annular Mode and Antarctic Peninsula Summer Temperatures: Analysis of a High-Resolution Model Climatology, Journal of Climate, 21, 1649-1668, 10.1175/2007JCLI1695.1, 2008.

~~New insights into the climatic signal from firn cores at the northern Antarctic Peninsula~~New regional insights into the stable water isotope signal at the northern Antarctic Peninsula as tools for climate studies

Francisco Fernandoy[1], Dieter Tetzner[2], Hanno Meyer[3], Guisella Gacitúa[4], Kirstin Hoffmann[3], Ulrike Falk[5]

[1]Facultad de Ingenieria, Universidad Andres Bello, Viña del Mar, 2531015, Chile
[2]Center for Climate and Resilience Research, Universidad de ~~ty of~~ Chile, Santiago, 8370361, Chile
[3]Alfred Wegener Institute Helmholtz Centre for Polar and Marine Research, Research Unit Potsdam, Telegrafenberg A43, 14473 Potsdam, Germany.
[4]Programa GAIA-Antártica, Universidad de Magallanes, Punta Arenas, 6210427, Chile
[5]Climate Lab, Geography Depart., University Bremen, 28334 Bremen, Germany

Correspondence to: Francisco Fernandoy (francisco.fernandoy@unab.cl)

Abstract. The Antarctic Peninsula is one of the most challenging regions of Antarctica from a climatological perspective, owing to the recent atmospheric and oceanic warming. The steep topography and a lack of long–term and in situ meteorological observations complicate extrapolation of existing climate models to the sub-regional scale. Here, we present new evidence from the northern Antarctic Peninsula to demonstrate how stable water isotopes of firn cores and recent precipitation samples can reveal climatic processes related to nearby oceanic and atmospheric conditions. A noticeable effect of the sea ice cover on local temperatures and atmospheric modes, in particular the Southern Annular Mode (SAM), is demonstrated. In years with large sea ice extension in winter (negative SAM anomaly), an inversion layer in the lower troposphere develops at the coastal zone. Therefore, an isotope–temperature relationship valid for all seasons cannot be concluded. The δ–T. relationship rather depends on seasonal variability of oceanic conditions. Transitional seasons (autumn and spring) are both stable seasons with an isotope–temperature gradient of +0.69‰ °C^{-1}. The firn stable isotope composition reveals that the near–surface temperature at the most northern portion of the Antarctic Peninsula shows a decreasing trend (-0.33°C y^{-1}) between 2008 and 2014. Moreover, the deuterium excess (d_{excess}) has been demonstrated to be a reliable indicator of seasonal oceanic conditions, and therefore suitable to improve a firn age model based on seasonal d_{excess} variability. The annual accumulation rate in this region is highly variable, ranging between 1060 kg m^{-2} y^{-1} and 2470 kg m^{-2} y^{-1} from 2008 to 2014. The combination of isotopic and meteorological data is key for reconstructing recent climatic conditions with a high temporal resolution in polar regions where no direct observation exists.

1 Introduction

West Antarctica and especially the Antarctic Peninsula (AP~~I~~) have been in the scope of the scientific community due to the notable effects of the present warming on the atmosphere, cryosphere, biosphere and ocean. The increase of air temperatures along the West Antarctic Peninsula coast (Carrasco, 2013) displays signs of a shifting climate system since the early 20th century (Thomas et al., 2009). Recently, rapid warming of both atmosphere and ocean is causing instability of ice shelves on West Antarctica, especially in some regions of the AP~~I~~ (Pritchard et al., 2012). The collapse of ice shelves triggers an accelerated ice–mass flow and discharge into the ocean, as the ice shelves' buttressing function gets lost. Several grounded tributary glaciers on AP~~I~~ and in West Antarctica recently loose mass to the oceans at accelerated rates due to this phenomenon (Pritchard and Vaughan, 2007; Rignot et al., 2005; Pritchard et al., 2012), which in combination with surface snow melt, has contributed to a negative surface mass balance especially in the northern part of the AP~~of the~~ region (Harig and Simons, 2015; Seehaus et al., 2015; Dutrieux et al., 2014; Shepherd et al., 2012).

The glacier of AP~~I~~ ~~is~~ have lost~~ing~~ ice mass at a rate of around 27 (±2) Gt year^{-1} between 2002 and 2014, which combined with the mass loss over West Antarctic~~a~~ ice sheet of 121(±8) Gt year^{-1}, surpassed~~s~~ the positive mass balance observed in East Antarctica (Harig and Simons, 2015). This demonstrates how sensitive the coastal region of West Antarctica is to ~~This demonstrates how sensitive the coastal region of West Antarctica reacts on~~ increased air and sea surface temperatures (Bromwich et al., 2013; Meredith and King, 2005).

Surface snow and ice melt ~~has significantly increased~~ on the AP~~I~~ ~~during the last decades,~~ represents~~ing~~ up to 20% of the total surface melt area (extent) and 66% of the melt volume of whole Antarctica for at least the last three decades (Trusel et al., 2012; Kuipers Munneke et al., 2012). Regional positive temperatures detected by remote sensing techniques and ice core data reveal that melt events have been temporally more wide–spread since the mid–20th century (Abram et al., 2013; Trusel et al., 2015), with some severe melt events during the first decade of the 21st century (Trusel et al., 2012). Increased surface melt and glacier calving may have an impact on the fresh water budget of the upper ocean layers and therefore on the biological activity of the coastal zone (Meredith et al., 2016; Dierssen et al., 2002). The most significant warming trend detected at the coast of the AP~~I~~ occurs during winter season, especially on the west side of the Peninsula, where a tendency >0.5°C decade^{-1} for the period 1960–2000 has been reported at~~for~~ several stations (Turner et al., 2005; Carrasco, 2013). Winter warming is especially evident on the daily minimum and monthly mean temperature increase, as described by Falk and Sala (2015) for the meteorological record of the Bellingshausen Station at King George Island (KGI) at the northern AP~~I~~ during the last 40 years. In KGI the daily mean temperature during winter increased at about 0.4°C decade^{-1}, with a~~highly~~ marked warming during August at a rate of +1.37(±0.3) °C decade^{-1}. Therefore, positive temperatures even in winter are more commonly observed, leading to more frequent and extensive surface melting year–round especially for the northern AP~~I~~, which is dominated by maritime climate conditions (Falk and Sala, 2015).

The mechanisms behind increasing atmosphere and ocean temperatures are still not completely understood but can be confidently linked to perturbations of regular (pre-industrial period) ~~typical~~ atmospheric circulation patterns (Pritchard et al., 2012; Dutrieux et al., 2014). Most heat advection to the southern ocean and atmosphere has been related to the poleward movement of the ~~southern oscillation or~~ Southern Annular Mode (SAM) and to some extent to the El Niño Southern Oscillation (ENSO) (Gille, 2008; Dutrieux et al., 2014; Fyfe et al., 2007). During the last decades, SAM has been shifting into a positive phase, implying lower than normal (atmospheric) pressures at coastal Antarctic regions (latitude 65°S) and higher (atmospheric) pressures over mid–latitudes (latitude 40°S) (Marshall, 2003). With lower pressures around Antarctica, the circumpolar westerly winds increase in intensity (Marshall et al., 2006). Air masses transported by intensified westerlies overcome the topography of the AP~~I~~ more frequently, especially in summer, bringing warmer air to the east side of the AP~~I~~ (van Lipzig et al., 2008; Orr et al., 2008). The relationship between the shift of the SAM and the surface air temperature trend is generally positive for the AP~~I~~, explaining a large part (~50%) of near–surface temperature increase for the last half century (Marshall et al., 2006; Marshall, 2007; Carrasco, 2013; Thompson and Solomon, 2002). An enhanced circulation allows more humidity to be transported to and trapped at the west coast of the AP~~I~~ due to the orographic barrier of the central mountain chain. Therefore, the accumulation has consistently increased across the entire Peninsula during the whole 20th century, doubling the accumulation rate from the 19th century in the southern AP~~I~~ region (Thomas et al., 2008; Goodwin et al., 2015; Dalla Rosa, 2013).

The increase of greenhouse gas concentrations and the stratospheric depletion of the ozone layer, both linked to anthropogenic activity, are suggested to be the main forcing factors of the climate shift that affects the ocean–atmosphere–cryosphere system for at least the last half century (Fyfe and Saenko, 2005; Sigmond et al., 2011; Fyfe et al., 2007).

The lack of long–term meteorological records hampers accurately determining ~~hampers to accurately determine~~ the onset and regional extent of this climate shift. Therefore, climate models are necessary to extend the scarce climate data both spatially and temporally ~~Therefore, climate models were improved and used to extend the scarce climate data both spatially and temporally~~. One major challenge is to correctly integrate the steep and rough topography of the AP~~I~~ into climate models. To realize this goal, direct information on surface temperature, melting events, accumulation rates, humidity sources and transport paths are urgently needed. As direct measurements of these parameters are not available, researchers must rely on the reconstruction of the environmental variability, mainly based on proxy data such as the stable water isotope composition of precipitation, firn and ice (e.g.:Thomas and Bracegirdle, 2009; Thomas et al., 2009; Abram et al., 2013).

In this investigation, we focus on a stable water isotope–based, high temporal resolution reconstruction (seasonal resolution between austral autumn 2008 and austral summer 2015) of variables including accumulation rates, temperatures and melt events on the AP~~I~~ and their relationship to atmospheric modes and moisture–source conditions i.e. sea surface temperature, humidity and sea ice extent.

Since 2008, we have undertaken several field campaigns to the northernmost region of the AP~~I~~, where we have retrieved a number of firn cores of up to 20 m depth. The present investigation is the first of it kinds for this portion of AP, other study has been carried out further south at Detroit Plateau (Dalla Rosa, 2013) and Bruce Plateau (Goodwin et al., 2015), at around 100 and 400 km South–West of the northern AP. Nonetheless the available glaciological and meteorological information for the study zone remains scarce. A more detailed description of the glaciological setting can be found in the work by Fernandoy et al. (2012). ~~-~~By using the stable water isotope composition of these cores as a proxy for the recent climate variability, we aim to fill the gap of lacking meteorological (in situ) observations. We have determined the effects of the orographic barrier of the AP~~I~~ on the air mass and moisture transport, with increasing precipitation rates from the coast to the mountain range on the Peninsula divide at ca. 1100 m a.s.l. (Fernandoy et al., 2012), where the ice thickness reaches ca. 350 m at its highest surface point (Cárdenas et al., 2014) .

2 Methodology

2.1 Field work and sample processing

During five austral summer campaigns (2008–2010, 2014, 2015)~~, several shallow depth firn cores (totaling more than 60 m) were retrieved from the northern part of the API. An~~ an altitudinal profile was completed from sea level near O´Higgins Station (OH) to 1130 m a.s.l at the Laclavere Plateau (LCL) (Fig. 1). In total, five firn cores were included in this paper: OH-4, OH-5, OH-6, OH-9, OH-10 (Fig. 1); coordinates and further details of the firn cores are given in Table 1. ~~More than 200~~210 daily precipitation samples were gathered at the meteorological observatory of the ~~from~~ O´Higgins Station (57.90°W, 63.32°S, 13 m a.s.l.) during 2008-2009 (Fernandoy et al., 2012) and 2014 (Table 2). From ~~Some of~~ these samples, around 6% (13 samples) were discarded from the analysis due to improper storing. This was evidenced by unusual values of stable water isotope analyses, and were discriminated using a statistical outlier test (modified Thompson tau technique). Cores OH-4, OH-5, OH-6 and OH-9 were retrieved between 2008 and 2010 and analyzed for their stable water isotope composition and physical properties of ice as described in Fernandoy et al. (2012) and Meyer et al. (2000). Additionally, a density profile of OH-9 was obtained by using an X-ray microfocus computer tomograph at the ice core processing facilities of the Alfred Wegener Institute, Helmholtz Centre for Polar and Marine Research in Bremerhaven, Germany (Linow et al., 2012). The X-ray tomography provides a very high–resolution (1mm) density profile of the physical properties of the ice. The core OH-10 was retrieved in 2015 using an electric drilling device with 5.7 cm inner diameter (Icedrill.ch AG). The retrieved core was first stored under controlled temperature conditions (-20°C) at the Chilean scientific station Prof. Julio Escudero (King George Island) and later transported to a commercial cold storage in Viña del Mar, Chile. The core sections were measured and weighted for density–profile construction and then sub–sampled with a 5 cm resolution for stable water isotope analysis. ~~.~~A visual logging and description of the cores were carried out to identify possible melt layers and their thicknesses. Thereafter, the samples were melted overnight at 4°C in a refrigerator at the Stable Isotope Laboratory of the Universidad Nacional Andrés Bello (UNAB), Viña del Mar, Chile. To avoid any evaporation, the 5cm samples were placed in sealed bags (Whirl-pak) and agitated for homogenization before isotopic analysis. ~~Thereafter, f~~Firn and recent precipitation samples collected from OH in 2014 (Table 1) were analyzed by a liquid water stable isotope analyzer from Los Gatos Research (TLWIA 45EP), ~~located~~ located at the UNAB facilities~~at the Stable Isotope Laboratory of the Universidad Nacional Andrés Bello, Viña del Mar, Chile~~. Accuracy of the measurements is better than 0.1 ‰ for oxygen and 0.8 ‰ for hydrogen isotopes for all samples analyzed. All oxygen and hydrogen stable water isotope data of precipitation and firn core samples are presented in relation to the Vienna Standard Mean Ocean Water Standard (VSMOW) in ‰, as $\delta^{18}O$ and δD for oxygen and hydrogen isotopes, respectively.

2.2 Database and time series analysis

Stable water isotope data were compared to major meteorological parameters from the region (Fig. 2). For this purpose, the following data sets were incorporated into our analysis: Near–surface air temperature (T_{air}), precipitation amount (Pp) and sea–level pressure (SLP), recorded at the Russian Station Bellingshausen (BE) (58.96°W, 62.19°S, 15.8 m a.s.l.), available in daily and monthly resolution from the Global Summary of the Day (GSOD) data sets of the National Climatic Data Center (NCDC, available at: www.ncdc.noaa.gov) and the SCAR Reference Antarctic Data for Environmental Research (READER, available at: https://legacy.bas.ac.uk/met/READER/~~www.antarctica.ac.uk/met/READER/~~) (Turner et al., 2004). Sea surface temperature (SST) time series were extracted from the Hadley Centre observation ~~Sea Ice and Sea Surface Temperature~~ data sets (Had~~I~~SST3, available at: ~~http://hadobs.metoffice.com/hadisst/~~http://www.metoffice.gov.uk/hadobs/hadsst3/). The Had~~I~~SST3 provides SST monthly means on a global 5° to 5° grid from 1850~~973~~ to present (Kennedy et al., 2011a, b) ~~(Rayner et al., 2003a)~~. Mean monthly SSTs were extracted from a quadrant limited by 60–65°S and 65–55°W. Missing data or outliers were interpolated from measurements taken in the neighbor quadrants. Relative humidity (*rh*) time series were extracted from data obtained by the calculation of 3 day air parcel backward trajectories under isobaric conditions using the freely–accessible Hybrid single-particle Lagrangian integrated trajectory (HYSPLIT) model (Draxler and Hess, 1998, available at: http://ready.arl.noaa.gov/HYSPLIT.php). This three–dimensional model was fed with the global data assimilation system (GDAS) archives from NOAA/NCEP (Kanamitsu, 1989). GDAS offers a global 1° to 1° latitude–longitude spatial coverage with a 1 hour temporal resolution and is available from 2006 to present (for more details visit: http://ready.arl.noaa.gov/gdas1.php). For studying the characteristics of air parcels approaching the AP~~I~~, *rh* time series were obtained considering data from 1 day backward trajectories arriving at isobaric conditions (850 hPa) over OH location. SST and *rh* datasets were resampled to a regional scale defined by high–density trajectory paths (Bellingshausen and Weddell Seas). The resampled fields were defined by the spatial coverage of 1 day backward trajectories. The limits of the resulting quadrant extends from 98° W to 34° W longitude and from 47° S to 76° S latitude. After noticing from air parcel backward trajectories the existence of a high density pathway and obtaining the conditions that prevail in the surroundings of AP~~I~~, we determined that the area covered by the tracks of 2 day backward trajectories was representative of the maritime conditions of this region. The representativeness of this area is because it geographically includes the region affected by westerly winds and sea ice front during winter time, both factors that exerts high influence on the air parcels that approach this region. A field horizontal mean of resampled *rh* values between sea level and 150 m a.s.l. was computed in this area to construct *rh* time series utilized throughout this work. Altitudinal temperature profiles were obtained from radiosonde measurements carried out at BE between 1979 and 1996 (SCAR Reference Antarctic Data for Environmental Research). Lapse rates were calculated from the temperature difference between sea level and the 850 hPa level. SAM index time series were obtained from the British

Antarctic Survey (BAS, available at: http://legacy.bas.ac.uk/met/gjma/sam.html) (Marshall, 2003). Mean monthly sea ice extent around the AP~~I~~ (between 1979 and 2014) was obtained from the Sea Ice Index from the National Sea & Ice Data Center (NSIDC, available at http://nsidc.org). The measurements of sea ice extension incorporated in this study considered as a starting point the coastal location of OH, and ~~as an end point,~~ the sea ice front in the direction towards KGI as an end point.

2.3 Stable Isotope time series analysis

The raw datasets obtained from stable water isotope analysis in firn cores were characterized for producing relatively flat isotope-~~/~~depth profiles. The isotope signals showed to be considerably noisy, with values fluctuating closely around the mean. Although there was a significant difference between the Standard Deviation (Sdev) values from lower altitude cores (OH-4, δ^{18}O Sdev =~~:~~ 1.2) and higher altitude cores (OH-10, δ^{18}O Sdev =~~:~~ 2.57) (Table 1), there were no clear detachments within each signal. The profiles described lacked of patterns which could be attributed by their own to seasonal cycles. Despite several attempts were carried out to achieve a chronology by annual layer counting, the noise and the lack of a consistent behavior in the signals inhibited this procedure. ~~The d~~Difficulties resulted~~arised~~ from using conventional dating methods with these firn cores~~,~~ led to the search for other types of methods that~~which~~ could provide a time frame to be compared with our signals. The relationship between the moisture source conditions and the isotopic signature of precipitations was further explored for~~with~~ this purpose.

For each precipitation event registered at OH, a 3 day air parcel backward trajectory was calculated ~~to identify *rh* conditions above sea level in the ocean near the API. For this purpose we used~~ using the HYSPLIT model with hourly temporal resolution. Frequent air parcel paths were studied and monthly mean values of *rh* and SST were calculated. Using the relationship between *rh* and SST calculated by Uemura et al. (2008), a theoretical value of deuterium excess ($d_{excess\ meteo}$) was calculated for the OH station and nearby area (i.e.: northern Antarctic Peninsula) ~~whole region~~ ($d_{excess\ meteo}$= -0.42 * rh + 0.45 * SST + 37.9). Comparisons were made between time series of deuterium excess (d_{excess}= δD - 8 * δ^{18}O), derived~~obtained~~ from monthly mean values of the precipitation isotopic signal, and $d_{excess\ meteo}$, obtained from monthly mean values of *rh* and SST from the southern oceans.

Simultaneously, the d_{excess} signal obtained from stable isotope analysis of firn cores was transformed into a signal depicted with depth. Then it was filtered using the Inverse Fast Fourier Transform (IFFT), which was fed with the frequency of the second of the principal modes of oscillation obtained from the Fast Fourier Transform (FFT). Thus, the final signal is only defined by the low frequencies. The same procedure was applied to the time series constructed with monthly means of $d_{excess\ meteo}$. The strong similarities between both signals, due to their dependency on the same variables, enables the transformation from the depth domain of the d_{excess} stable isotope signal to the time domain by using the common principal oscillation patterns as time markers. As d_{excess} is now represented in the time domain (Fig. 3), monthly means were calculated to generate time series for further analysis. Once the d_{excess} signals from firn cores were represented as time series, the same procedure was followed to generate δ^{18}O time series (Fig. 3). The δ^{18}O – Temperature relationship was obtained from precipitation samples and daily mean temperatures at OH.

2.4 Complementing geophysical data

Ground–penetrating radar (GPR) is a geophysical method based on the propagation and reflection of electromagnetic waves (Annan and Davis, 1976). Reflections are produced when dielectric discontinuities are reached in the propagation media. GPR has been proven~~d~~ to be effective in dry snow layer interpretation where reflections are most commonly produced from internal density differences (Spikes et al., 2004). Therefore, GPR data complement ice–core interpretations, allowing the spatial extrapolation of ice–core layer detection and evaluation of layer continuity.

GPR measurements were performed during the OH-10 firn core drilling campaign in January 2015. We used a SIR3000 unit equipped with a 400 MHz central frequency antenna (GSSI Inc.), - that was dragged in a sledge along the proposed measurement lines (Fig. 4). The penetration depth of the electromagnetic waves is strongly controlled by the electrical conductivity of the propagation medium (i.e. snow) as well as by the central frequency of the system (Daniels, 2007), which decreases as frequency increases. The used system provides a good compensation between these parameters, where the vertical resolution in dry polar snow is approximately 0.35 m reaching up to 100 m in depth (Spikes et al., 2004). However, these values are variable for snow/firn in low polar latitudes (e.g. Antarctic Peninsula), where the range for layer detection increases and the maximum depth decreases.

Raw radar data were processed and interpreted using the software Reflexw (http://www.sandmeier-geo.de). Each radar profile was manually georeferenced using differential global positioning system (DGPS) data collected during the GPR measurements. Prior to the snow/firn stratigraphy interpretation from radar imaging, processes and corrections included removal of repetitive traces and application of filters to diminish signal noise (e.g. frequency filter, deconvolution and stacking). Each collected file was analyzed independently and layers were distinguished and chosen manually~~. Thus, if layers were not sufficiently clear and continuous, the files were not picked~~ (Fig. 5). Data was further analyzed in the ASCII format (i.e. *easting*, *nothing*, *elevation*, *depth*).

3. Results

~~Oxygen and hydrogen stable water isotope data of precipitation and firn core samples are presented in relation to the Vienna Standard Mean Ocean Water Standard (VSMOW) in ‰, as δ^{18}O and δD for oxygen and hydrogen isotopes, respectively.~~

3.1 Precipitation samples ~~OH~~

Table 2 and Fig. 6 show~~s~~ the stable isotope results,~~ and~~ basic statistics and annual distribution of~~for~~ the precipitation samples collected at OH station, respectively. The comparison between δD and δ^{18}O from precipitation samples allows the definition of a Local Mean Water Line (LMWL) given by the expression $\delta D = 7.83 * \delta^{18}O - 0.12$. Backward trajectory analysis for precipitation events reveals a high–frequency transport across the Bellingshausen Sea within the last 24 hours before the air parcels reach the AP~~I~~ (Fig. 7~~6~~).

3.1.1 Isotope ~~–~~— Temperature relationship

Using the stable water isotope composition of single precipitation events and daily near–surface temperature (T_{daily}), an isotope–temperature relationship was constructed for OH station using a linear regression analysis. For this purpose, each season~~s~~'s sample set was selected from the months with the largest number of samples (i.e. December 2008, March 2008 and~~–~~—2009, June 2008 and October 2014). The purpose was~~is,~~ mainly to ensure having the larger dataset within a short period of time that could evidence if there was coherence and relation between $\delta^{18}O$~~–~~—T. All comparisons between $\delta^{18}O$ and T_{daily} revealed correlation coefficients (R) higher than 0.6 and a statistical significance (*p*) lower than 0.03 for a total of 208 precipitation events analyzed. Outliers were discarded as explained in section 3.1.2. Furthermore, the same analysis was carried out using monthly averages calculated from daily events ($T_{monthly}$) from the whole precipitation dataset (R= 0.5, p= 0.01), considering a total of 24 months. Considerable differences were identified between the daily and monthly $\delta^{18}O$~~–~~—T relationships (Fig. 6~~7~~a). The linear regression slope (*s*) of austral—autumn or MAM (March-April-May), considering the March 2008 and~~–~~—2009 dataset to be representative of the MAM behavior, has shown to be quite near to *s* of austral summer or SON (September-October-November), considering the October 2014 dataset to be representative of the SON behavior: s= 0.77 (standard error= 2.08, p<0.01) and s= 0.61 (standard error= 2.88, p=0.03), respectively. If only the two datasets (MAM and SON) are taken into account, a new linear regression can be obtained as: $\delta^{18}O= 0.69* T_{daily}+4.43$ (R= 0.74, p<0.01). Thus, the time series of monthly averages shows a direct relation between both parameters. An inverse behavior of *s* was identified during July 2008 and June 2014, compared to MAM and SON. Following the same procedure, austral summer season or DJF (December-January-February) was represented by the sample set of December 2008 and austral winter or JJA (June-July-August) was represented by the sample set of June 2008, with *s* values of 1.17 (standard error= 0.62, p=0.~~,~~01) and 0.35 (standard error= 1.74, p<0.01), respectively. Additionally, mean seasonal lapse rates obtained in this region show the higher values towards DJF (-5.31 °C~~/~~ km^{-1}), similar values during MAM and SON (4.43°C ~~/~~km^{-1}, and -4.06°C ~~/~~km^{-1} respectively) and the lowest values during JJA (-2.73° ~~C~~/km^{-1}) (Fig. 8).

3.1.2 Deuterium excess ~~–~~— Temperature relationship

From stable water isotope results obtained from precipitation samples, d_{excess} values were calculated for each sample. Table 2 shows d_{excess} basic statistics for the dataset. The d_{excess} values lower than -9~~2.0~~ ‰ and higher than 12 ‰ (see Section 2.1) were filtered in order to avoid disturbances, as these samples might have been influenced by secondary processes during storage and transport. Daily d_{excess} values for the same months as specified in section 3.1.1 were compared with daily mean temperatures. Correlation coefficients for these comparisons are not significant~~weak~~ (R<-0.42, p>0.1) and broadly scattered. The comparison considering monthly averages calculated from daily events from the whole dataset improved the d_{excess}~~–~~—T correlation coefficient (R= -0.71, p<0.01; T= -0.98 * d_{excess} - 0.33) (Fig. 6~~7~~b). Time series of monthly averages show a clear inverse relationship between both parameters for the whole dataset.

3.1.3 Moisture source of precipitation

Air backward trajectories from precipitation events exhibit a wide spatial distribution, including the South Pacific Ocean and the Amundsen~~–~~–Bellingshausen Seas. The trajectories are mainly distributed in the Bellingshausen Sea, the Bransfield Straight and the Drake Passage, partially including Tierra del Fuego and South America's southern tip, although some trajectories (<15%) originate from AP~~I~~'s eastern side. Precipitation trajectories show an almost N40°W elliptically distributed pattern where most of them follow pathways restricted between latitudes 60°S and 67°S. From the relationship between monthly mean values of d_{excess} from precipitation samples and $d_{excess\ meteo}$ constructed from meteorological parameters (*rh* and SST) of the high density precipitation pathways, a correlation coefficient of R= 0.86 (p<0.01) was obtained (Fig. 9~~8~~).

3.2 Firn core samples from AP~~I~~

Table 1 shows the stable isotope results and basic statistics for firn cores retrieved at the northern AP~~I~~. The co–isotopic relationship δD~~–~~– $\delta^{18}O$ of each single firn cores retrieved from LCL is close to the global meteoric water line (GMWL) ~~(Rozanski et al., 1993)~~ and the local meteoric water line (LMWL) (Rozanski et al., 1993), with a mean slope of ~~m~~s= 7.91 and an intercept of 3.64 (Fig. 10~~9~~). These values are very close to those of the LMWL, although with a slightly higher intercept.

3.2.1 Age model based on stable water isotope~~ and geophysical data~~

Stable water isotope results from firn cores allowed us to derive depth profiles of δD, $\delta^{18}O$ and d_{excess} for each firn core. Lower noise and the clearest seasonal pattern was found in d_{excess} profiles ($d_{excess\ core}$) (Fig. 3), similar to findings published by Fernandoy et al. (2012). The $d_{excess\ core}$ signals were analyzed by filtering their high frequency oscillation patterns and comparing the remnant signals with $d_{excess\ meteo}$ monthly means, which prevail on the high density pathways, covered by air parcels that reach LCL surroundings within 2 days. Main peak–valley fitting between both signals led to a monthly mean $d_{excess\ core}$ signal represented on a time scale. The comparison between time series of monthly mean $d_{excess\ core}$ and $d_{excess\ meteo}$ data reveals correlation coefficients of R≥0.67 (p<0.01) for all firn cores analyzed and obtained from 2006 to 2015. Table 3 summarizes correlation coefficients, statistical significances and time intervals covered by each firn core. From the firn cores retrieved from LCL, a single time series was constructed and then compared to the $d_{excess\ meteo}$ time series in order to analyze the isotopic signal along the whole time interval. A correlation coefficient of R= 0.75 (p<0.01) was obtained between the two signals ($d_{excess\ meteo}$ and $d_{excess\ core}$). To construct one single time series from the firn cores, on the overlapping time interval between OH-9 and OH-10 (February 2012 to January 2014), we only considered data from OH-9, because the samples from OH-9 consists of more fresh and less compacted firn than the respective interval in OH-10. This in turn helps to avoid attenuation of the isotopic signal. Although we only considered OH-9 data for the overlapping time interval, we studied the changes in the standard deviation of the isotopic signal in both firn cores in the common time span. The standard deviation shows a decrease of 16% after one year of deposition in core OH-10 with respect to the same time interval in OH-9; and 2 to 3 years after the deposition the smoothing of the signal increased up to 18%.

During firn core visual logging, thin and scarce melt layers were identified (mean width of ~1 cm). The melt layers do not show evidence of infiltration nor have a clear pattern of distribution with depth (i.e. association with summer layers). While analyzing them in relation to their time equivalent with depth, no clear pattern associated with a season was noted.

3.2.2 Seasonal temperature reconstruction from stable water isotope ratios

The age model developed using the $d_{excess\ core}$ oscillation was later applied to construct a $\delta^{18}O$ time series (Fig. 3). From this time series a periodical 2 year pattern was identified. This pattern is characterized by elevated values, higher than the $\delta^{18}O$ monthly mean~~s,~~ between May and November in the years 2008, 2010, 2012 and 2014, which exhibit an inverse relationship to temperature at BE. Between June and July in the following years 2009, 2011 and 2013, $\delta^{18}O$ values are lower than the mean and exhibit a direct relationship to temperature at BE (Fig. 11~~0~~). Monthly mean $\delta^{18}O$ values were transformed to their temperature equivalent using the $\delta^{18}O$ ~~=~~– T relationship obtained in section 3.1.1 from precipitation samples (Fig. 12~~1~~)~~.~~ ~~Monthly $\delta^{18}O$ =– T relationship was considered to reflect seasonal behavior~~. As calendar seasonal behavior in these latitudes does not play a significant role and seasonality is able to extend beyond calendar limits, we defined three seasons with their correspondent ~~differences were found to be more pronounced during different years, for those cases the use of certain~~ $\delta^{18}O$ ~~=~~– T relationship. These seasons are: an austral transitional season ~~were extended or contracted considering~~ which considers months from March to May and October-November (MAM-ON) (considers precipitation datasets from March 2008~~=~~–2009 and~~,~~ October 2014 for the $\delta^{18}O$~~=~~–T relationship), an austral winter season which considers month between June and September (JJAS) (considers precipitation datasets from June 2008 for the $\delta^{18}O$~~=~~–T relationship), and an austral summer season which considers months from December to February (DJF) (considers precipitation datasets from December 2008 for the $\delta^{18}O$~~=~~–T relationship). Despite this main seasonal classification for the use of $\delta^{18}O$~~=~~–T relationship, some particular seasons showed variable behavior when they were compared to the mean seasonal behavior in the time span covered in this study~~with respect to the general trend~~tendency ~~during specific years~~. In those cases, the seasonal behavior was extended or contracted beyond the boundaries of the main season classification depending on sea ice extent. Large sea ice extent during winter, will lead to a delayed on~~=~~–set of spring conditions. In this case winter~~=~~–like conditions will be extended beyond August. Restricted sea ice extent on the contrary will lead to earlier spring~~=~~–like conditions (before August).

Additionally, the relationship between monthly lapse rates in BE, winter SAM index and sea ice extent (SIE) from OH is represented in Fig. 13~~2a~~. As temperature data from OH show several large record gaps, for the estimation of air temperature on LCL, we considered the BE temperature corrected by a latitude ~~factor~~ difference (-1.4°C) (see section 2.2). The BE data was considered for this calculation because of the high correlation with OH ($r= 0.97$, $p<0.01$) and long term consistency of the data (uninterrupted record since 1968). The correction is given by the linear regression between OH and BE temperature data. Other nearby stations like Esperanza (63.40°S, 57.00°W), were not considered because a slight lower correlation ($r= 0.96$, $p< 0.01$) and likely continental influence over the temperature record. Considering latitude–corrected air temperatures from BE, lapse rates from BE and SIE from OH (SIE_{OH}), a mean annual air temperature of -7.5°C with a trend of -0.18°C $year^{-1}$ (statistically not significant at p=0,05) was estimated on LCL for the time period 2009-2014 ~~(Fig. 12b)~~. A monthly temperature mean estimate, derived from the linear correlation between meteorological data and the monthly ~~$\delta^{18}O$~~ lapse rate~~–~~–SIE~~T~~ relationship, can be expressed by the equation $T_{LCL}= (T_{BE} -1.4)+1.13\ (M_{month}*SIE_{OH}+N_{month})$, during the months when sea ice is developed (from May to September) and where M_{month} and N_{Month} represent the slope and intercept of the monthly lapse rate ~~–~~–SIE ~~$\delta^{18}O$ – T~~ relationship, respectively. During the months when there is no sea ice (from October to April) the monthly temperature can be expressed by the equation $T_{LCL}= (T_{BE} -1.4)+1.13 * ~~(~~H(t)~~)~~$, where H(t) is the monthly mean lapse rate value of the month ~~"~~t~~"~~ measured in BE between 1978-1996. Additionally, considering the $\delta^{18}O$ time series data and the isotope~~–~~–T relationship, a mean annual air temperature of -6.5°C with a trend of -0.33°C year^{-1} (statistically not significant at p=~~<~~0.05) was estimated on LCL for the years 2009-2014. The comparison between monthly mean temperature on LCL, estimated using the $\delta^{18}O$ signal from firn cores and T_{LCL} estimated using the coupled effect of the latitude–corrected temperature record from BE, SIE_{OH} and lapse rates from BE, reveals a correlation coefficient of R= 0.7 (p<0.01). Both signals show a synchronous behavior, also with respect to the air temperature record at OH station. No statistically significant direct correlation was observed between coastal stations (OH and BE) temperature records and the stable water isotope composition of ~~-~~firn cores. Comparing the $\delta^{18}O$ signal from OH-6 with data from precipitation samples at OH and with two other cores from the western side of the AP~~I~~ (OH-4 and OH-5) during a common period (March 2008 – August 2008), a $\delta^{18}O$ decrease of -0.085‰ km^{-1} was found with increasing distance from the coast (Fig.~~ure~~ 14~~3~~a). The same data set was used to study the $\delta^{18}O$~~–~~–altitude relationship. The $\delta^{18}O$ seasonal means show altitude dependence through which seasonal $\delta^{18}O$~~–~~–altitude patterns could be distinguished. During MAM a clear decreasing rate of -2.4‰ km^{-1} from sea level up to LCL is found, whereas during JJA no ~~clear~~ decreasing $\delta^{18}O$ trend is obtained from sea level up to 1130 m a.s.l. (Fig.~~ure~~ 14~~3~~b).

3.2.3 Accumulation rates

Density measurements from firn cores were used to construct density~~–~~–depth profiles. Along those profiles a significant~~clear trend of~~ increas~~e~~ing of density with depth was obtained. Linear regressions across different sections represent a normal firn compaction process reaching the snow~~–~~–firn~~–~~–density boundary (550 kg ~~c~~m^{-3}) at 15.2 m depth. Using these linear regressions and considering the depth intervals delimited in section 3.2.1 as monthly values, we were able to estimate accumulation rates during different periods. By using this procedure, we have estimated accumulation rates at LCL between 2008 and 2015, with a mean accumulation of 1770 kg m^{-2} y^{-1}. The highest value was found in 2008 (>2470 kg m^{-2}), then the accumulation rate noticeably decreased until 2015 (1600 kg m^{-2}) reaching its lowest absolute value in 2010 (1060 kg m^{-2}) (Fig. 15~~4~~a). A seasonal trend was observed, reflecting a decrease in the accumulation during JJA and SON between 2008 and 2015, which is responsible for the overall decreasing rates. On the other hand, the highest accumulation occurs during MAM and SON seasons (Table 4). Accumulation rate estimations derived from cores OH-9 and OH-10 for 2012 – 2013 (common period) differ only by about 3%. Other cores from the west flank of the Peninsula (OH-4, OH-5 and OH-6) show that the accumulation in 2008 (common period) depends on the altitude, with increasing values from the lower region to the highest point on LCL (Fig. 15~~4~~b). The increase rate is about 1500 kg m^{-2} km^{-1} y^{-1} from 350 m a.s.l. to 1130 m a.s.l.

3.2.4 GPR data interpretation around OH-10 site

~~GPR electromagnetic waves are reflected from the dielectric interfaces produced when seasonal snow is accumulated (Arcone, 2009). However, low compaction between recent years of accumulated snow at LCL prevented the detection of snow stratigraphy in depths less than ~7 m. The minimum depth of a continuous layer observed was 7.4 m and the deepest layer reached up to 41.8 m below the surface.~~

~~Wind circulation from the northwest cause wind erosion and thus hamper layer detection. Therefore, layer density and continuity were less visible at the northwest side. The minimum number of detected layers by GPR section was 9, and the maximum was 16 (Figure 5). Referring to the isotope–based dating of the OH-10 core, the GPR signal indicates that at the OH-10 site, 7.4 m of accumulated snow corresponds to January 2013. Consequently, the deepest layer detected corresponds to the austral summer of 1998 (~41 m snow/firn accumulation in 16 years).~~GPR electromagnetic waves are reflected from the dielectric interfaces produced when seasonal snow is accumulated (Arcone, 2009). However, low compaction between recent years of accumulated snow at LCL prevented the identification of stratigraphy in the upper snowpack (less than ~9 m).

Wind fluxes from the northwest cause that layer density and continuity were less visible on this side of the prospected area. Since layer interpretation was only performed where distinct continuous horizons were clearly visible, the layer detection was further analysed comparing interpretation of the radar profiles to determine if layers were consistently recognized. This analyses resulted in 17 layers detected upon 42 ± 0.6 m of snow accumulation. Layers depth were estimated using a 2D wave velocity model based on a combination of local ice core density (less than 15 m) observations and a comparable density model used from Bruce Plateau core for deeper snow (Goodwin, 2013).

Referring to the isotope–based dating of the OH-10 core, the GPR signal indicates that at the OH-10 site, the first layer detected (10.9 ±1.5 m) corresponds to January 2012. Consequently, the deepest layer detected corresponds to the austral summer of 1995 resulting in an average annual accumulation of 1122 ± 59 kg m^{-2} y^{-1} for this period (mean density 614 kg m^{-3}).

4 Discussion

4.1 Stable water isotope fractionation processes and the local temperature relationship

The stable water isotope compositions of precipitation samples from the 2008 and 2014 datasets show a high similarity to each other, as well as to firn cores from the western flank and from LCL Plateau at AP~~I~~ (OH-4 to OH-10), and to several meteorological and climatic parameters and reanalysis data. Backward trajectory analysis revealed that the most frequent pathways for air parcels that reach the northern part of AP~~I~~ derive from the Bellingshausen Sea, between 55°S and 60°S (Fig. 7~~6~~) throughout the year. In contrast, localities further south on the AP~~I~~ and in West Antarctica, Ellsworth Land and coastal Ross Sea, respectively, exhibit a stronger continental influence on the precipitation source, depending on seasonal and synoptic scale conditions (Thomas and Bracegirdle, 2015; Sinclair et al., 2012). The LMWL obtained from precipitation samples at OH (m= 7.83) is closely related to the Antarctic meteoric water line obtained by Masson-Delmotte et al. (2008) (m= 7.75), and to the GMWL as presented by Rozanski et al. (1993) (m= 8.13). The similarity between the slope of LMWL and GMWL indicates that the fractionation processes during condensation mostly take place under thermodynamic equilibrium (Moser and Stichler, 1980). These results are consistent with those obtained by other authors for King George Island (Simões et al., 2004; Jiahong et al., 1998). Moreover, by combining the stable water isotope signature of OH precipitation with time series of meteorological data representative for the conditions prevailing on the ocean near OH station, a strong relationship with *rh* and SST at the moisture source can be derived. This relationship has been well established, especially for the coastal Antarctic region where moisture transport from the source is generally short–ranging (Jouzel et al., 2013). The comparison between the d_{excess} of precipitation and the theoretical $d_{excess\ meteo}$ derived from time series of meteorological data from the surrounding region has shown that both datasets are highly correlated (R= 0.86). Based on this evidence, we suggest that the Bellingshausen Sea constitutes the most important source of water vapor for precipitation for~~at the~~ ~~AP~~the study region at the northern AP~~I~~. A similar conclusion was found for regions further south in the Peninsula (Thomas and Bracegirdle, 2015), however, with an increase of other local sources (e.g.: Amundsen Sea and continental conditions) to the local precipitation. This could be also observed at the northern AP, where ~~S~~some precipitation events that exhibited a stable water isotope composition beyond the normal range for the region (e.g. 20 August 2009, $\delta^{18}O$ = -19.4‰), ~~-~~were associated with uncommon sources of humidity as also recognized by the backward trajectory analysis.

The changing seasonal $\delta^{18}O$–T relationship obtained from precipitation samples shows that the relationship between air temperature and condensation temperature varies throughout the year. The strong similarity in the $\delta^{18}O$–T relationship during MAM and SON contrasts with the pronounced difference of this relationship between DJF and JJA. This highlights the variability of the $\delta^{18}O$–T relationship along the whole year at the northern AP~~ in this region~~. Although the $\delta^{18}O$–T relations, presented in this study, were calculated from precipitation samples of particular months and years, which can certainly induce to some bias, to consider those datasets give a rough idea of the variations that can be seen in between seasons in this area. Furthermore, the $\delta^{18}O$–T relationships obtained for MAM and SON (0.77‰ °C^{-1}and 0.61‰ °C^{-1}, respectively) are similar to the values obtained by other authors for the API (Aristarain et al., 1986; Peel et al., 1988). Even though the considered dataset can be capable of representing variations within the time span covered by this study, it is too limited to build a consistent baseline for the region.~~Nonetheless, the $\delta^{18}O$–T relationships obtained for MAM and SON (0.77‰ °C^{-1} and 0.61‰ °C^{-1}, respectively) are similar to the values obtained by other authors for the API (Aristarain et al., 1986; Peel et al., 1988).~~ Despite~~Although~~ the seasonal temperature difference is reduced in coastal sites, the difference in the seasonal $\delta^{18}O$–T relationship suggests the existence of processes that disrupt the direct linkage between condensation temperature and surface air temperature. The inverse relationship between the $\delta^{18}O$ signal from LCL ice cores and BE (and OH) monthly mean temperatures (Fig. 12~~1~~), which is noticeable in some years during JJA, contrasts with the commonly accepted seasonal behavior characterized by a direct relationship between $\delta^{18}O$ and surface air temperatures (Clark and Fritz, 1997). This particular behavior could be related to strong variations in meteorological conditions in the area between BE (OH) and LCL throughout the whole year. Therefore, air temperature on LCL was estimated by two independent methods: lapse rates (vertical temperature gradient) and $\delta^{18}O$ – T equivalents. The best correlation between both temperatures was obtained when an extended seasonal behavior was considered (R= 0.7; $p<0.01$). This result is in agreement with the natural seasonal variability in high latitudes, where the effects of some seasons extend beyond the theoretical seasonal temporal limits, as previously explained. Failing to take this seasonal variability into account would lead to a misinterpretation of the air temperature reconstruction for LCL, since then the $\delta^{18}O$~~–~~—T correlation would be rather poor (R= 0.42) and would not reflect the true seasonality in this region. The high similarity in $\delta^{18}O$—T relationship during MAM and SON can be explained by the seasonal transition between summer and winter, when oceans surrounding the northern AP~~I~~ pass from ice–free to fully ice–covered conditions, respectively. Likely, ice–free ocean conditions are related to ~~natural~~ seasonal oscillations, which are highly dependent on atmospheric circulation patterns. In this sense, years with a marked negative SAM anomaly are associated with ice–covered sea conditions, whereas positive SAM phases are associated with ice–free sea conditions (Fig. 13~~2~~). Other studies (Turner et al., 2016) point to a similar interaction between surface air temperature and SIE at AP~~I~~ and recognized that the SIE's inter–annual variability is related to atmospheric modes. This supports our own observations in a way that the sea ice is important for regulation of surface air temperatures in the region.

In firn cores obtained from AP~~I~~, mean $\delta^{18}O$ and δD values show a decreasing tendency~~rend~~ with increasing height from sea level up to LCL (1130 m a.s.l.), which provides evidence for the altitudinal effect identified by Fernandoy et al. (2012). In addition, standard deviation of seasonal (monthly mean) δD and $\delta^{18}O$ values of firn cores from LCL is low and similar to that of the firn cores from lower altitudes. Despite the variations in isotopic composition with height, in all firn cores the δD~~–~~— $\delta^{18}O$ co~~–~~—isotopic relation is very similar to the LMWL obtained from precipitation samples at OH. This provides evidence of the uniformity of the fractionation conditions during the condensation process. Although a slight isotopic smoothing effect was distinguished between the cores (16% after one year of deposition), the distortions caused by post~~–~~-depositional effects that may alter or homogenize the isotopic signal at this site, such as diffusion, can be considered as limited. The latter indication is well supported by the high accumulation rate in the region that does not allow a prolonged exposition of the freshly fallen snow to the atmosphere. Furthermore, the absence of significant infiltration and percolation associated with melting and refreezing events and the lack of a relationship between ice layers and the stable water isotope record implies ~~that the formation of melt layers is~~ that the isotopic composition is not altered by surface melt infiltration and percolation ~~not related to variations in the isotopic signal obtained from firn cores.~~ Thus, this reassures that post–depositional processes in the LCL region are negligible in the time period analyzed and that ice layers likely developed by wind ablation on wind–scouring processes at the plateau. Although these observations are in agreement with the results obtained in this region by Fernandoy et al. (2012) and Aristarain et al. (1990), several studies (Fernandoy et al., 2012; Simões et al., 2004; Travassos and Simoes, 2004; Jiahong et al., 1998) have identified a significant amount of melt layers in firn cores, mainly from KGI and from the western side of the AP~~I~~ at altitudes below 700 m a.s.l. The limited effect of post~~–~~—depositional processes due to the high accumulation rates and to the ice layers reducing diffusion (Stichler et al., 2001), along with the high correlation between $d_{excess\ meteo}$ and d_{excess} obtained from firn cores, confirm that the isotopic variations observed in firn core isotope records are mostly related to isotopic fractionation occurring during condensation and to *rh* and SST conditions in the vapor source regions.

4.2 Firn age model and accumulation rates

The stable water isotope signal obtained from firn cores shows no regularity in its seasonal behavior and lacks a clear annual oscillation pattern, possibly because of the strong maritime influence (Clark and Fritz, 1997). These two criteria prevent the development of an age model by conventional annual layer counting in the isotope record (Legrand and Mayewski, 1997). In this context, the d_{excess} parameter represents a robust time indicator, as it has shown to be principally dependent on *rh* and SST conditions prevailing in the eastern Bellingshausen Sea where these variables are relatively stable (Jouzel et al., 2013). The high correlation coefficients (and high statistical significance) obtained for the relationship between d_{excess} and $d_{excess\ meteo}$, as shown in section 3.2.1, demonstrate that the method used to construct time series is effective in dating isotope records of firn cores from the northern AP~~I~~, even at a monthly resolution.

The most frequent d_{excess} values found in the firn cores (3‰ – 6‰) are in agreement with a strong coastal influence scenario as determined by Petit et al. (1991), implying that the d_{excess} relates to *rh* and SST of the humidity source and not to surface air temperature (Jouzel et al., 2013). Saigne and Legrand (1987), postulated that *rh* conditions prevailing at the sea surface have an important effect on the d_{excess} signal of precipitation below 2000 m a.s.l in the study region. The stable water isotope results, in combination with the meteorological records presented in this work, show that precipitation on LCL is highly correlated with *rh* and SST conditions in the Bellingshausen Sea near the AP~~I~~.

The irrelevance of post–depositional effects along with the flat topography on LCL suggests that the estimate of accumulation rates from firn cores is representative of the amount of snow originally precipitated. Moreover, the slight smoothing of the isotope signal effect after deposition along with only small differences in the accumulation rate observed for the common time period of firn cores OH-9 and OH-10, demonstrates that our age model is reliable, as two different data sets yield similar estimations for a common period. The results obtained allow to classify LCL as a high annual snow accumulation site (Table 4), closely following the estimations of other authors on King George Island dome (Bintanja, 1995; Zamoruyev, 1972; Jiahong et al., 1998) and on the AP~~I~~ further south of LCL (Dalla Rosa, 2013; Goodwin, 2013; van Wessem et al., 2015), of around 2000 – 2500 kg m^{-2} y^{-1}, but differs from the accumulation rate obtained by Simões et al. (2004) and Jiankang et al. (1994) on King George Island dome (600 kg m^{-2} y^{-1}). A seasonal bias of the accumulation was noted, with more favorable conditions for accumulation (i.e. higher precipitation amount) during autumn resulting from more synoptic scale features approaching the AP~~I~~ (Table 4).

4.3 Seasonal variability and disruption of atmospheric conditions

The depletion of $\delta^{18}O$ with increasing height (altitude effect) and the simultaneous increase in accumulation along the western side of AP~~I~~ at LCL latitude can be explained with the help of an orographic precipitation model as proposed by Martin and Peel (1978). This model states that moist air parcels from the Southern Ocean are forced to ascend and cool down when approaching the AP~~I~~ due to the steep topography forming an orographic barrier to westerly winds. The depletion observed in $\delta^{18}O$ could reflect the strength of the fractionation process taking place within a short distance and in a low temperature environment (Fig. 16~~5~~a). Therefore, the isotopic fractionation process occurring along the AP~~I~~ and the direct linear relation between δ^{18}O and condensation temperature allow us to study the temperature behavior with respect to the altitude increase on the basis of δ^{18}O variations (Craig, 1961). However, whereas MAM air temperatures show a clear decrease with increasing height (atmospheric instability of the lower troposphere), JJA air temperatures exhibit an inverse pattern (an increase) from sea level up to 350 m a.s.l (atmospheric stability). At higher altitudes, a decreasing temperature trend is observed (atmospheric instability). The break at 350 m a.s.l during JJA indicates the existence of a strong stratification within the lower troposphere on the western side of the AP~~I~~. In addition, the variations in monthly mean lapse rates measured by radiosondes in BE throughout the year, provide evidence for the existence of a process that modifies the behavior of the lower troposphere, decreasing the lapse rate (between sea level and 850 hPa) during JJA and considerably increasing it during DJF (Fig. 17~~6~~). The close linear relationship identified between lapse rate magnitude and SIE indicates that SIE is an important factor for the development of these variations between May and September.

The phenomena previously described is likely linked to the development of an inversion layer in the lower troposphere on the western side of the AP~~I~~ mainly during JJA, which in turn is related to a strong radiative imbalance. During JJA, solar radiation diminishes until it reaches a minimum at the winter solstice. The lack of solar radiation leads to considerable cooling that favors the formation of sea ice and in turn, causes differential cooling between the sea ice surface and the air above it. As the sea ice surface cools faster than the air above it, a near–surface altitudinal pattern of increasing temperature develops where local atmospheric stability prevails. The layer of atmospheric stability extends from sea level up to at least 350 m a.s.l, where it turns into an atmospheric instability regime. Both regimes together favor the decrease of the overall lapse rate, as temperature first increases and then decreases with height. Conversely, no inversion layer is formed during DJF due to the absence of sea ice and hence, atmospheric instability prevails, which is related to high lapse rates (Fig. 16~~5~~b and 16~~5~~c).

The existence of an inversion layer during the months with sea ice coverage might explain the low oscillation of monthly mean temperatures estimated at LCL compared to monthly mean air temperatures at BE (OH). The inverse relation between SAM index and SIE also seems to play an important role, as SAM positive phases enhance the transport of warm and moist air towards the western side of the AP~~I~~, thus inhibiting the formation of sea ice. This has a direct impact on the lapse rate as the development of an inversion layer is hindered and therefore air temperatures on LCL are regulated. The interaction between SAM and SIE plays a key role as sea–ice–covered conditions temper the maritime system, favoring continental–like conditions and reducing annual mean air temperature, implying a higher temperature amplitude in BE and OH throughout the year.

The temperature time series estimated from the stable water isotope record (δ^{18}O and d_{excess}) from LCL firn cores exhibits a periodic (biannual) pattern, which can be linked to a similar periodical behavior observed in SAM index and in SIE. The relatively constant temperatures observed during MAM, JJA and SON in years with a positive SAM phase provide evidence that during these seasons condensation is taking place at similar temperatures. Under such conditions (positive SAM), the low variations in the lapse rate throughout the year, along with the low thermal oscillation in BE (OH) explain the presence of a constant condensation temperature, which does not differ much from air temperature during DJF. Conversely, the stronger annual temperature oscillation observed on LCL during negative SAM phases indicates marked variations in condensation temperature throughout the year.

Finally, the proposed inversion layer model (Fig. 17~~6~~) explains the seasonal variations observed in the $\delta^{18}O$~~—~~T relationship of precipitation samples from OH. The distortion of the direct relation between condensation temperature and surface air temperature by an inversion layer makes it necessary to differentiate $\delta^{18}O$~~—~~T relationship according to the lapse rate evolution throughout the year. In this context, MAM and SON were identified as transitional periods in the formation of the inversion layer, mainly because of the sea–ice formation and retreat during these seasons. The seasonal adjustment considered to estimate LCL temperatures must be applied~~ mainly~~, because the sea–ice cover varies inter–annually in its duration and extension, which in turn produces the inter–annually variable inversion layer. The proposed model for the coastal region on the western side of the AP~~I~~ at OH latitude, is consistent with the observations of Yaorong et al. (2003) on KGI (South Shetland Islands), through which the development of several inversion layers that extend beyond 400 m a.s.l.

5 Conclusions

In this study, we examined one of the most complete records of recent precipitation from the northern AP~~I~~, with a total of 210 single precipitation events and more than 60 m of firn cores. The firn cores retrieved in this work include the accumulation at the northwestern AP~~I~~ region between 2008~~6~~ and 2014 from. Precipitation and firn stable water isotope compositions have been compared to different meteorological data sets to determine their representativeness as climate proxies~~y~~ for the region.

The results of our study reveal significant seasonal changes in the $\delta^{18}O$~~—~~T relationship throughout the year. For autumn and spring a $\delta^{18}O$–T ratio of 0.69‰ °C^{-1} (r= 0.74) was found to be most representative, whereas for winter and summer the $\delta^{18}O$–T ratio appears to be highly dependent on SIE conditions. The apparent moisture source for air parcels precipitating at the northern AP~~I~~ is mainly located in the Bellingshausen Sea and in the southern Pacific Ocean. The transport of water vapor along these oceanic and coastal pathways exerts a strong impact on the d_{excess} signal of precipitation. The comparison between the d_{excess} signal from the moisture source and the d_{excess} signal from firn cores has proved to be a successful method for dating firn cores from the northern AP~~I~~, delivering a seven–year isotopic time series in high temporal resolution for LCL.

Based on our dating method we could define LCL as a high snow accumulation site, with a mean annual accumulation rate of 1770 kg m^{-2} y^{-1} for the period 2006–2014. However, accumulation is highly variable from year to year, with a maximum and minimum of 2470 kg m^{-2} (in 2008) and 1060 kg m^{-2} (in 2010), respectively. In addition, we identified the presence of a strong orographic precipitation effect along the western side of the AP~~I~~ reflected by an accumulation increase with altitude (1500 kg m^{-2} y^{-1} km^{-1}), as well as by the isotopic depletion of precipitation from sea level up to LCL (-2.4‰ km^{-1} for autumn) and from the coast line up to the ice divide (-0.08 ‰ km^{-1}).

The maritime regime present on the western side of the AP~~I~~ has a strong control on air temperatures, observed as restricted summer/winter oscillation, and is reflected in a poor seasonality of the $\delta^{18}O$ and δD profiles in firn cores. Recent climatic conditions can be reconstructed from $\delta^{18}O$ time series obtained from LCL firn cores only when considering an inversion layer model during winter season. The strength of the inversion layer likely depends on SIE and SAM index values. Taking into account the effect of the inversion layer on the isotope–temperature relationship, we observe a slight cooling trend of mean annual air temperature at LCL with an approximate rate of -0.33°C y^{-1} for the period sampled by the examined firn cores (2009-2014). This finding is in line with evidence from stacked meteorological record of the nearby research stations as determined by Turner et al. (2016).

Our results demonstrate that the stable water isotope composition of firn cores retrieved from LCL is capable of reproducing the meteorological signal present in this region, validating it as a valuable proxy for paleo–climate reconstructions in the northern AP~~I~~ region. Environmental (atmosphere and ocean) and glaciological conditions present at LCL, a ~350 m thick ice cap, together with an almost undisturbed isotopic record are optimal prerequisites for the preservation of a climate proxy record with a high temporal resolution. Consequently, LCL is a suitable site for recovering a medium–depth ice core to investigate climate variations during the last centuries in the northern AP~~I~~ region.

6 Acknowledgements

The present work was funded by the FONDECYT project 11121551 and supported by the Chilean Antarctic Institute (INACH), the Chilean Air Force and Army logistic facilities. We want to show our gratitude to the Universidad Nacional Andres Bello for supporting this study. We also greatly thank our colleagues, who made field work conditions less severe, especially to Daniel Rutllant for his support on the logistic and field safety. ~~Finally, w~~We would like to thank all people involved on the laboratory work, especially to Ivonne Quintanilla, who carried out the sample processing at UNAB and to Dr. Johannes Freitag, for his support with the X-Ray tomography processing at AWI. Tracy Wormwood is greatly thanked for her support editing this manuscript. We highly appreciate the comments of two anonymous reviewers, who provided helpful observations that greatly contributed to improve this manuscript. Finally, we thank the dedicated work of the editor of this article Benjamin Smith.

References

Abram, N. J., Mulvaney, R., Wolff, E. W., Triest, J., Kipfstuhl, S., Trusel, L. D., Vimeux, F., Fleet, L., and Arrowsmith, C.: Acceleration of snow melt in an Antarctic Peninsula ice core during the twentieth century, Nature Geosci, 6, 404-411, doi: 10.1038/ngeo1787, 2013.

Annan, A. P., and Davis, J. L.: Impulse radar sounding in permafrost, Radio Science, 11, 383-394, doi: 10.1029/RS011i004p00383, 1976.

Arcone, S. A.: Glaciers and Ice Sheets, in: Ground Penetrating Radar Theory and Applications, First edition ed., edited by: Jol, H. M., Elsevier Science, Amsterdam, 361-392, 2009.

Aristarain, A., Jouzel, J., and Pourchet, M.: Past Antarctic Peninsula climate (1850-1980) deduced from an ice core istope record, Climatic Change, 9, 69-89, 1986.

Aristarain, A., Jouzel, J., and Lorius, C.: A 400 Year Isotope record of the Antarctic Peninsula climate, Geophys. Res. Lett., 17, 2369-2372, doi: 10.1029/GL017i013p02369, 1990.

Bintanja, R.: The local surface energy balance of the Ecology Glacier, King George Island, Antarctica: measurements and modelling, Antarctic Science, 7, 315-325, doi: 10.1017/S0954102095000435, 1995.

Bromwich, D. H., Nicolas, J. P., Monaghan, A. J., Lazzara, M. A., Keller, L. M., Weidner, G. A., and Wilson, A. B.: Central West Antarctica among the most rapidly warming regions on Earth, Nature Geosci, 6, 139-145, doi: 10.1038/ngeo1671, 2013.

Cárdenas, C., Johnson, E., Fernandoy, F., Meyer, H., Cereceda, F., and Vidal, V.: Preliminary results of the superficial and sub-glacier topography survey using Radio Echo Sounding at the La Claveré Plateau, Antarctic Peninsula, SCAR Open Science Conference, Auckland, New Zealand, 1-3 September, 2014.

Carrasco, J. F.: Decadal Changes in the Near-Surface Air Temperature in the Western Side of the Antarctic Peninsula, Atmospheric and Climate Sciences, 03, 7, doi: 10.4236/acs.2013.33029, 2013.

Clark, I., and Fritz, P.: Environmental Isotopes in Hydrogeology, edited by: Stein, J., and Starkweather, A., Lewis, Boca Raton, New York, 311 pp., 1997.

Craig, H.: Isotopic variations in meteoric waters, Science, 133, 1702-1703, doi: 10.1126/science.133.3465.1702, 1961.

Dalla Rosa, J.: Variabilidade da taxa de acumulação de neve no Platô Detroit, Península Antártica, M.S. thesis, Instituto de Geociências, Universidade Federal do Rio Grande do Sul, Porto Alegre, 98 pp., 2013.

Daniels, D. J.: Ground penetrating radar, 2nd ed., IET Radar, Sonar, Navigation and Avionics, 15, The Institution of Engineering and Technology, Herts, United Kingdom, 2007.

Dierssen, H. M., Smith, R. C., and Vernet, M.: Glacial meltwater dynamics in coastal waters west of the Antarctic peninsula, Proceedings of the National Academy of Sciences, 99, 1790-1795, doi: 10.1073/pnas.032206999, 2002.

Draxler, R. R., and Hess, G. D.: An Overview of the HYSPLIT-4 modelling system for trajectories, dispersion and deposition, Aust. Meterol. Mag., 47, 295-308, 1998.

Dutrieux, P., De Rydt, J., Jenkins, A., Holland, P. R., Ha, H. K., Lee, S. H., Steig, E. J., Ding, Q., Abrahamsen, E. P., and Schröder, M.: Strong Sensitivity of Pine Island Ice-Shelf Melting to Climatic Variability, Science, 343, 174-178, doi: 10.1126/science.1244341, 2014.

Falk, U., and Sala, H.: Winter melt conditions of the inland ice cap on King George Island, Antarctic Peninsula, Erkunde, 69, 341-363, doi: 10.3112/erdkunde.2015.04.04, 2015.

Fernandoy, F., Meyer, H., and Tonelli, M.: Stable water isotopes of precipitation and firn cores from the northern Antarctic Peninsula region as a proxy for climate reconstruction, The Cryosphere, 6, 313-330, doi: 10.5194/tc-6-313-2012, 2012.

Fyfe, J. C., and Saenko, O. A.: Human-Induced Change in the Antarctic Circumpolar Current, Journal of Climate, 18, 3068-3073, doi: 10.1175/JCLI3447.1, 2005.

Fyfe, J. C., Saenko, O. A., Zickfeld, K., Eby, M., and Weaver, A. J.: The Role of Poleward-Intensifying Winds on Southern Ocean Warming, Journal of Climate, 20, 5391-5400, doi: 10.1175/2007JCLI1764.1, 2007.

Gille, S. T.: Decadal-Scale Temperature Trends in the Southern Hemisphere Ocean, Journal of Climate, 21, 4749-4765, doi: 10.1175/2008JCLI2131.1, 2008.

Goodwin, B. P.: Recent Environmental Changes on the Antarctic Peninsula as Recorded in an ice core from the Bruce Plateau, Ph.D. thesis, Graduate Program in Atmospheric Science, Ohio State University, 247 pp., 2013.

Goodwin, B. P., Mosley-Thompson, E., Wilson, A. B., Porter, S. E., and Sierra-Hernandez, M. R.: Accumulation Variability in the Antarctic Peninsula: The Role of Large-Scale Atmospheric Oscillations and Their Interactions, Journal of Climate, 29, 2579-2596, doi: 10.1175/JCLI-D-15-0354.1, 2015.

Harig, C., and Simons, F. J.: Accelerated West Antarctic ice mass loss continues to outpace East Antarctic gains, Earth and Planetary Science Letters, 415, 134-141, doi: 10.1016/j.epsl.2015.01.029, 2015.

Jiahong, W., Jiancheng, K., Jiankang, H., Zichu, X., Leibao, L., and Dali, W.: Glaciological studies on the King George Island ice cap, South Shetland Islands, Antarctica, Annals of Glaciology, 27, 105-109, doi: 10.3198/1998AoG27-1-105-109, 1998.

Jiankang, H., Jiancheng, K., Jiahong, W., Lluberas, A., and Rodriguez, F.: General characteristics in stratigraphy and density variation for ice cores from Collins Ice Cap, King George Island, Antarctica, Antarctic Research, 6, 40-46, 1994.

Jouzel, J., Delaygue, G., Landais, A., Masson-Delmotte, V., Risi, C., and Vimeux, F.: Water isotopes as tools to document oceanic sources of precipitation, Water Resources Research, 49, 7469-7486, doi: 10.1002/2013WR013508, 2013.

Kanamitsu, M.: Description of the NMC Global Data Assimilation and Forecast System, Weath. Forecast., 4, 335-342, doi: 10.1175/1520-0434(1989)004<0335:DOTNGD>2.0.CO;2, 1989.

Kennedy, J. J., Rayner, N. A., Smith, R. O., Parker, D. E., and Saunby, M.: Reassessing biases and other uncertainties in sea surface temperature observations measured in situ since 1850: 1. Measurement and sampling uncertainties, Journal of Geophysical Research: Atmospheres, 116, n/a-n/a, 10.1029/2010JD015218, 2011a.

Kennedy, J. J., Rayner, N. A., Smith, R. O., Parker, D. E., and Saunby, M.: Reassessing biases and other uncertainties in sea surface temperature observations measured in situ since 1850: 2. Biases and homogenization, Journal of Geophysical Research: Atmospheres, 116, n/a-n/a, 10.1029/2010JD015220, 2011b.

Kuipers Munneke, P., Picard, G., van den Broeke, M. R., Lenaerts, J. T. M., and van Meijgaard, E.: Insignificant change in Antarctic snowmelt volume since 1979, Geophysical Research Letters, 39, doi: 10.1029/2011GL050207, 2012.

Legrand, M., and Mayewski, P.: Glaciochemistry of polar ice cores: A review, Rev. Geophys., 35, 219-243, doi: 10.1029/96RG03527, 1997.

Linow, S., Hörhold, M. W., and Freitag, J.: Grain-size evolution of polar firn: a new empirical grain growth parameterization based on X-ray microcomputer tomography measurements, Journal of Glaciology, 58, 1245-1252, doi: 10.3189/2012JoG11J256, 2012.

Marshall, G. J.: Trends in the Southern Annular Mode from observations and Reanalyses, J. Climate, 16, 4134-4143, doi: 10.1175/1520-0442(2003)016<4134:TITSAM>2.0.CO;2, 2003.

Marshall, G. J., Orr, A., van Lipzig, N. P. M., and King, J. C.: The Impact of a Changing Southern Hemisphere Annular Mode on Antarctic Peninsula Summer Temperatures, J. Climate, 19, 5388-5404, doi: 10.1175%2FJCLI3844.1, 2006.

Marshall, G. J.: Half-century seasonal relationships between the Southern Annular Mode and Antarctic temperatures, Int. J. Climatol., 27, 373-383, doi: 10.1002/Joc.1407, 2007.

Martin, P. J., and Peel, D. A.: The Spatial Distribution of 10 m Temperatures in the Antarctic Peninsula, Journal of Glaciology, 20, 311-317, doi: 10.3198/1978JoG20-83-311-317, 1978.

Masson-Delmotte, V., Hou, S., Ekaykin, A., Jouzel, J., Aristarain, A., Bernardo, R. T., Bromwich, D., Cattani, O., Delmotte, M., Falourd, S., Frezzotti, M., Gallée, H., Genoni, L., Isaksson, E., Landais, A., Helsen, M. M., Hoffmann, G., Lopez, J., Morgan, V., Motoyama, H., Noone, D., Oerter, H., Petit, J. R., Royer, A., Uemura, R., Schmidt, G. A., Schlosser, E., Simoes, J. C., Steig, E. J., Stenni, B., Stievenard, M., van den Broeke, M. R., van de Wal, R. S. W., van de Berg, W. J., Vimeux, F., and White, J. W. C.: A Review of Antarctic Surface Snow Isotopic Composition: Observations, Atmospheric Circulation, and Isotopic Modeling, J. Climate, 21, 3359-3387, doi: 10.1175%2F2007JCLI2139.1, 2008.

Meredith, M., and King, J. C.: Rapid climate change in the ocean west of the Antarctic Peninsula during the second half of the 20th century, Geophys. Res. Lett., 32, 1 - 5, doi: 10.1029/2005GL024042, 2005.

Meredith, M. P., Stammerjohn, S. E., Venables, H. J., Ducklow, H. W., Martinson, D. G., Iannuzzi, R. A., Leng, M. J., van Wessem, J. M., Reijmer, C. H., and Barrand, N. E.: Changing distributions of sea ice melt and meteoric water west of the Antarctic Peninsula, Deep Sea Research Part II: Topical Studies in Oceanography, doi: 10.1016/j.dsr2.2016.04.019, 2016.

Meyer, H., Schönicke, L., Wand, U., Hubberten, H. W., and Friedrichsen, H.: Isotope Studies of Hydrogen and Oxygen in Ground Ice - Experiences with the Equilibration Technique, Isot. Enviro. Healt. S., 36, 133 - 149, doi: 10.1080/10256010008032939, 2000.

Moser, H., and Stichler, W.: Environmental isotopes in ice and snow, in: Handbook of environmental isotope geochemistry, edited by: Fritz, P., and Fontes, J. C., Elsevier, New York, 141-178, 1980.

Orr, A., Marshall, G. J., Hunt, J. C. R., Sommeria, J., Wang, C.-G., van Lipzig, N. P. M., Cresswell, D., and King, J. C.: Characteristics of Summer Airflow over the Antarctic Peninsula in Response to Recent Strengthening of Westerly Circumpolar Winds, Journal of the Atmospheric Sciences, 65, 1396-1413, 10.1175/2007JAS2498.1, 2008.

Peel, D. A., Mulvaney, R., and Davison, B. M.: Stable-Isotope/Air-Temperature relationship in ice cores from Dolleman Island and the Palmer Land Plateau, Antarctic Peninsula, Ann. Glaciol., 10, 130-136, doi: 10.3198/1988AoG10-130-136, 1988.

Petit, J. R., White, J. W. C., Young, N. W., Jouzel, J., and Korotkevich, Y. S.: Deuterium Excess in Recent Antarctic Snow, J. Geophys. Res-Atmos., 96, 5113-5122, doi: 10.1029/90JD02232, 1991.

Pritchard, H. D., and Vaughan, D. G.: Widespread acceleration of tidewater glaciers on the Antarctic Peninsula, J. Geophys. Res., 112, F03S29, doi: 10.1029/2006jf000597, 2007.

Pritchard, H. D., Ligtenberg, S. R. M., Fricker, H. A., Vaughan, D. G., van den Broeke, M. R., and Padman, L.: Antarctic ice-sheet loss driven by basal melting of ice shelves, Nature, 484, 502-505, doi: 10.1038/nature10968, 2012.

Rayner, N. A., Parker, D. E., Horton, E. B., Folland, C. K., Alexander, L. V., Rowell, D. P., Kent, E. C., and Kaplan, A.: Global analyses of sea surface temperature, sea ice, and night marine air temperature since the late nineteenth century, J. Geophys. Res-Atmos., 108, 4407, doi: 10.1029/2002jd002670, 2003a.

Rayner, N. A., Parker, D. E., Horton, E. B., Folland, C. K., Alexander, L. V., Rowell, D. P., Kent, E. C., and Kaplan, A.: Global analyses of sea surface temperature, sea ice, and night marine air temperature since the late nineteenth century, Journal of Geophysical Research: Atmospheres, 108, 10.1029/2002JD002670, 2003b.

Rignot, E., Casassa, G., Gogineni, S., Kanagaratnam, P., Krabill, W., Pritchard, H., Rivera, A., Thomas, R., Turner, J., and Vaughan, D.: Recent ice loss from the Fleming and other glaciers, Wordie Bay, West Antarctic Peninsula, Geophys. Res. Lett., 32, L07502, doi: 10.1029/2004GL021947, 2005.

Rozanski, K., Araguás-Araguás, L., and Gonfiantini, R.: Isotopic Patterns in Modern Global Precipitation, in: Climate Change in Continental Isotopic Records, edited by: Swart, P. K., Lohman, K. C., McKenzie, J., and Savin, S., American Geophysical Union, Washington, USA, 1993.

Saigne, C., and Legrand, M.: Measurements of methanesulphonic acid in Antarctic ice, Nature, 330, 240-242, doi: 10.1038/330240a0, 1987.

Seehaus, T., Marinsek, S., Helm, V., Skvarca, P., and Braun, M.: Changes in ice dynamics, elevation and mass discharge of Dinsmoor–Bombardier–Edgeworth glacier system, Antarctic Peninsula, Earth and Planetary Science Letters, 427, 125-135, doi: 10.1016/j.epsl.2015.06.047, 2015.

Shepherd, A., Ivins, E. R., A, G., Barletta, V. R., Bentley, M. J., Bettadpur, S., Briggs, K. H., Bromwich, D. H., Forsberg, R., Galin, N., Horwath, M., Jacobs, S., Joughin, I., King, M. A., Lenaerts, J. T. M., Li, J., Ligtenberg, S. R. M., Luckman, A., Luthcke, S. B., McMillan, M., Meister, R., Milne, G., Mouginot, J., Muir, A., Nicolas, J. P., Paden, J., Payne, A. J., Pritchard, H., Rignot, E., Rott, H., Sørensen, L. S., Scambos, T. A., Scheuchl, B., Schrama, E. J. O., Smith, B., Sundal, A. V., van Angelen, J. H., van de Berg, W. J., van den Broeke, M. R., Vaughan, D. G., Velicogna, I., Wahr, J., Whitehouse, P. L., Wingham, D. J., Yi, D., Young, D., and Zwally, H. J.: A Reconciled Estimate of Ice-Sheet Mass Balance, Science, 338, 1183-1189, doi: 10.1126/science.1228102, 2012.

Sigmond, M., Reader, M. C., Fyfe, J. C., and Gillett, N. P.: Drivers of past and future Southern Ocean change: Stratospheric ozone versus greenhouse gas impacts, Geophysical Research Letters, 38, doi: 10.1029/2011GL047120, 2011.

Simões, J., Ferron, F., Bernardo, R., Aristarain, A., Stievenard, M., Pourchet, M., and Delmas, R.: Ice core study from the King George Island, South Shetlands, Antarctica., Pesquisa Antártica Brasileira, 4, 9-23, 2004.

Sinclair, K. E., Bertler, N. A. N., Trompetter, W. J., and Baisden, W. T.: Seasonality of Airmass Pathways to Coastal Antarctica: Ramifications for Interpreting High-Resolution Ice Core Records, Journal of Climate, 26, 2065-2076, doi: 10.1175/JCLI-D-12-00167.1, 2012.

Spikes, V. B., Hamilton, G. S., Arcone, S. A., Kaspari, S., and Mayewski, P. A.: Variability in accumulation rates from GPR profiling on the West Antarctic plateau, Annals of Glaciology, 39, 238-244, doi: 10.3189/172756404781814393, 2004.

Stichler, W., Schotterer, U., Fröhlich, K., Ginot, P., Kull, C., Gäggeler, H., and Pouyaud, B.: Influence of sublimation on stable isotope records recovered from high-altitude glaciers in the tropical Andes, J. Geophys. Res., 106, doi: 10.1029/2001jd900179, 2001.

Thomas, E. R., Marshall, G. J., and McConnell, J. R.: A doubling in snow accumulation in the western Antarctic Peninsula, Geophys. Res. Lett., 35, 1-5, doi: 10.1029/2007GL032529, 2008.

Thomas, E. R., and Bracegirdle, T. J.: Improving ice core interpretation using in situ and reanalysis data, J. Geophys. Res., 114, D20116, doi: 10.1029/2009jd012263, 2009.

Thomas, E. R., Dennis, P. F., Bracegirdle, T. J., and Franzke, C.: Ice core evidence for significant 100-year regional warming on the Antarctic Peninsula, Geophys. Res. Lett., 36, -, doi: 10.1029/2009gl040104, 2009.

Thomas, E. R., and Bracegirdle, T. J.: Precipitation pathways for five new ice core sites in Ellsworth Land, West Antarctica, Climate Dynamics, 44, 2067-2078, doi: 10.1007/s00382-014-2213-6, 2015.

Thompson, D. W. J., and Solomon, S.: Interpretation of Recent Southern Hemisphere Climate Change, Science, 296, 895-899, 10.1126/science.1069270, 2002.

Travassos, J., and Simoes, J.: High-resolution radar mapping of internal layers of a subpolar ice cap, King George Island, Antarctica, Pesquisa Antártica Brasileira, 4, 57-65, 2004.

Trusel, L. D., Frey, K. E., and Das, S. B.: Antarctic surface melting dynamics: Enhanced perspectives from radar scatterometer data, Journal of Geophysical Research: Earth Surface, 117, doi: 10.1029/2011JF002126, 2012.

Trusel, L. D., Frey, K. E., Das, S. B., Karnauskas, K. B., Kuipers Munneke, P., van Meijgaard, E., and van den Broeke, M. R.: Divergent trajectories of Antarctic surface melt under two twenty-first-century climate scenarios, Nature Geosci, 8, 927-932, 10.1038/ngeo2563 http://www.nature.com/ngeo/journal/v8/n12/abs/ngeo2563.html#supplementary-information, 2015.

Turner, J., Colwell, S. R., Marshall, G. J., Lachlan-Cope, T. A., Carleton, A. M., Jones, P. D., Lagun, V., Reid, P. A., and Iagovkina, S.: The SCAR READER project: Toward a high-quality database of mean Antarctic meteorological observations, J. Climate, 17, 2890-2898, doi: 10.1175/1520-0442(2004)017<2890:TSRPTA>2.0.CO;2, 2004.

Turner, J., Colwell, S. R., Marshall, G. J., Lachlan-Cope, T. A., Carleton, A. M., Jones, P. D., Lagun, V., Reid, P. A., and Iagovkina, S.: Antarctic climate change during the last 50 years, Int. J. Climatol., 25, 279-294, doi: 10.1002/joc.1130, 2005.

Turner, J., Lu, H., White, I., King, J. C., Phillips, T., Hosking, J. S., Bracegirdle, T. J., Marshall, G. J., Mulvaney, R., and Deb, P.: Absence of 21st century warming on Antarctic Peninsula consistent with natural variability, Nature, 535, 411-415, doi: 10.1038/nature18645, 2016.

Uemura, R., Matsui, Y., Yoshimura, K., Motoyama, H., and Yoshida, N.: Evidence of deuterium excess in water vapor as an indicator of ocean surface conditions, J. Geophys. Res., 113, 1-10, doi: 10.1029/2008JD010209, 2008.

van Lipzig, N. P. M., Marshall, G. J., Orr, A., and King, J. C.: The Relationship between the Southern Hemisphere Annular Mode and Antarctic Peninsula Summer Temperatures: Analysis of a High-Resolution Model Climatology, Journal of Climate, 21, 1649-1668, 10.1175/2007JCLI1695.1, 2008.

van Wessem, J. M., Reijmer, C. H., van de Berg, W. J., van den Broeke, M. R., Cook, A. J., van Ulft, L. H., and van Meijgaard, E.: Temperature and Wind Climate of the Antarctic Peninsula as Simulated by a High-Resolution Regional Atmospheric Climate Model, Journal of Climate, 28, 7306-7326, doi: 10.1175/JCLI-D-15-0060.1, 2015.

Yaorong, H., Zhenhe, X., and Cong, X.: A Study on Snowstorm Weather in Coastal Area of Western Antarctic, Marine Science Bulletin, 5, 24-31, 2003.

Zamoruyev, V. V.: Results of glaciological observations at Bellingshausen station in 1968, Trudy Sovetskoy Antarkticheskoy Ekspeditsii, 55, 135-144, 1972.

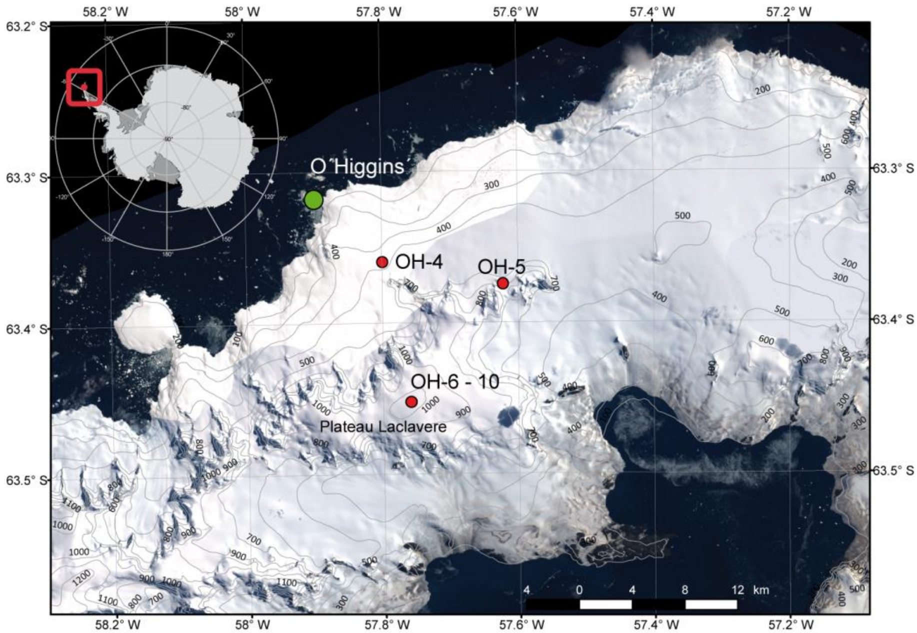

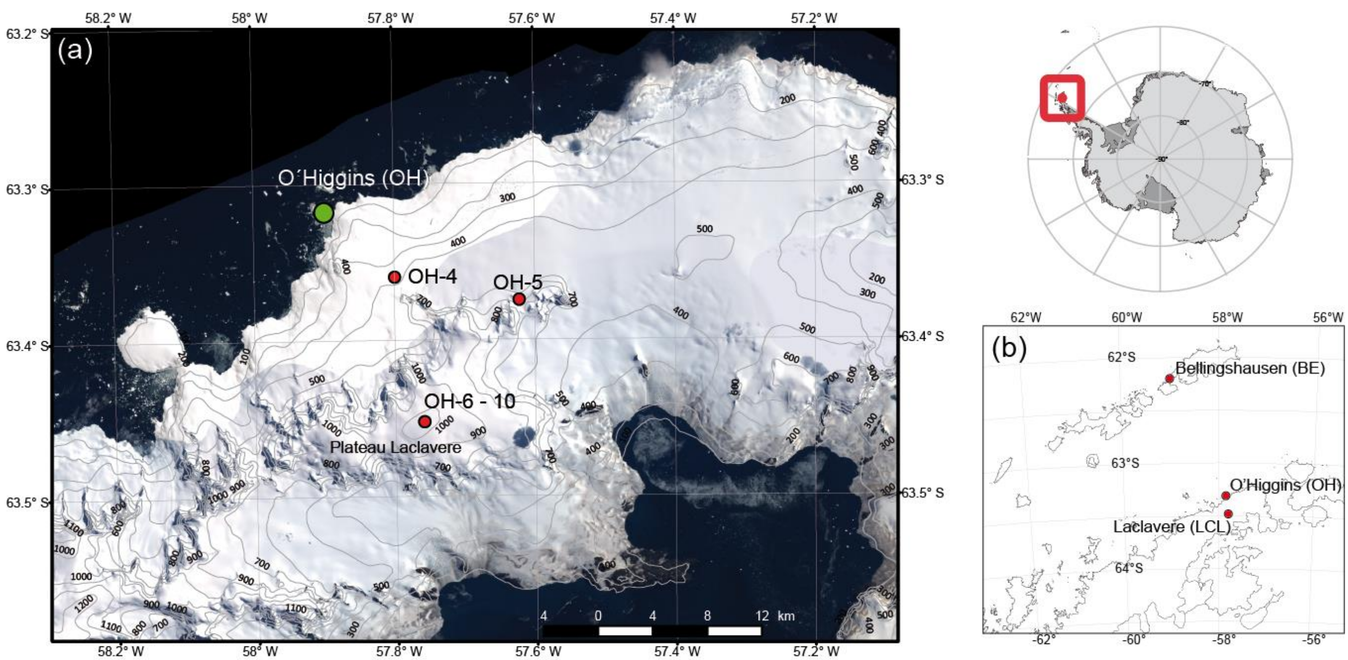

Figure 1: Investigation area and location of the firn cores presented in this work. (a) Detail of the study zone: ~~T~~the green point shows the Chilean Station O'Higgins (OH) at the west coast of the Antarctic Peninsula. Firn cores retrieved between 2008 and 2015 are shown by red dots. (b) Location of O'Higgins and Bellingshausen Station and Laclavere Plateau, which are mentioned through the text. Satellite image (Landsat ETM+) and digital elevation model (RADARSAT) available from the Landsat Image Mosaic of Antarctica (LIMA) (http://lima.usgs.gov/).

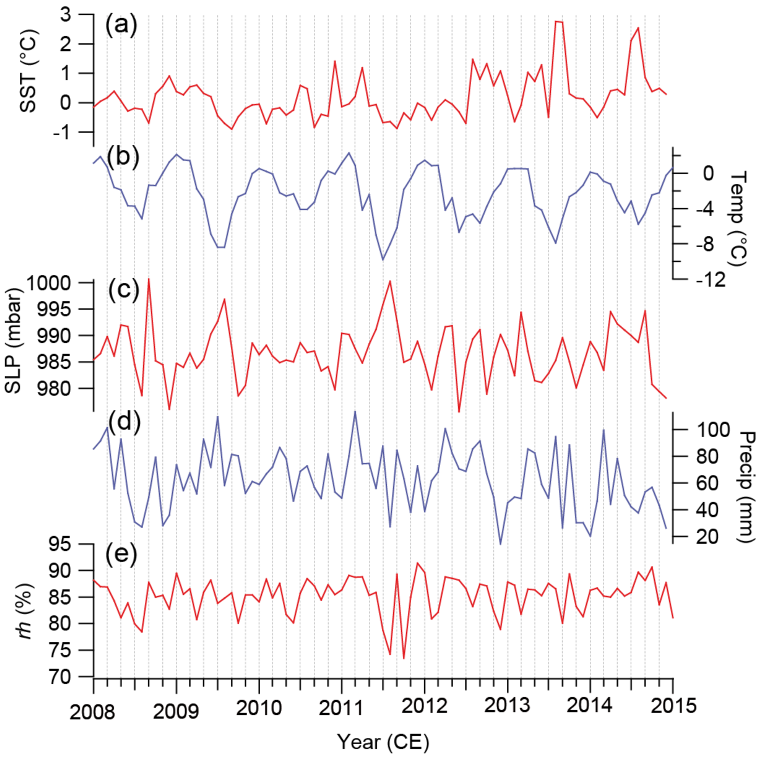

Figure 2: Meteorological data sets used in this study, (a) Sea surface temperature (SST), (b) Air temperature (Temp), (c) Sea level pressure (SLP) and (d) Precipitation amount (Precip) from Bellingshausen Station (BE) on King George Island and (e) Relative humidity (*rh*) from the Southern Ocean surrounding the northern Antarctic Peninsula (AP~~I~~) region. Data shown in the figure is available from the READER dataset (https://legacy.bas.ac.uk/met/READER/) (Turner et al., 2004).

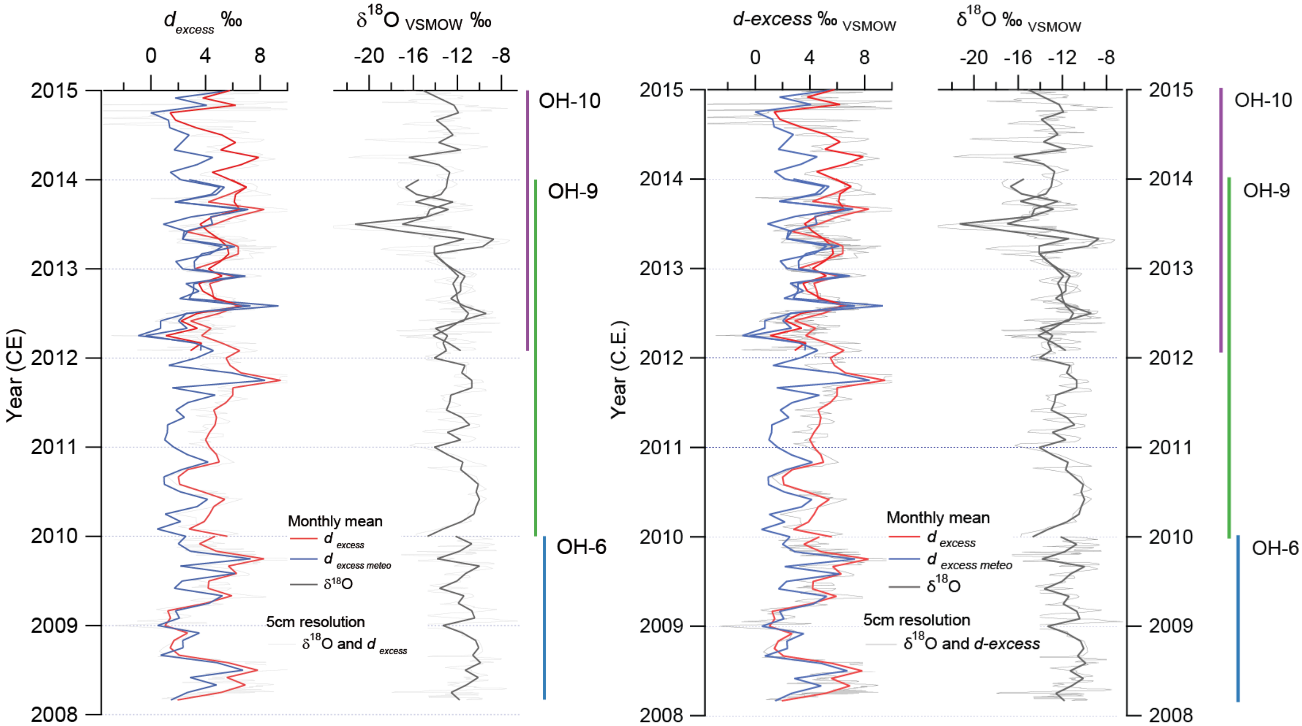

Figure 3: Time series for firn cores OH-6 (light blue line right), OH-9 (green light right) and OH-10 (purple line right) derived for $\delta^{18}O$ (black line right) and d_{excess} (red line left) records using a theoretical d_{excess} ($d_{excess\ meteo}$) value (blue line left). The $d_{excess\ meteo}$ is calculated from Sea surface temperature (SST) and Relative Humidity (*rh*) according to Uemura et al. (2008). All three cores are located at the same location within the GPS navigator horizontal error (<10m).

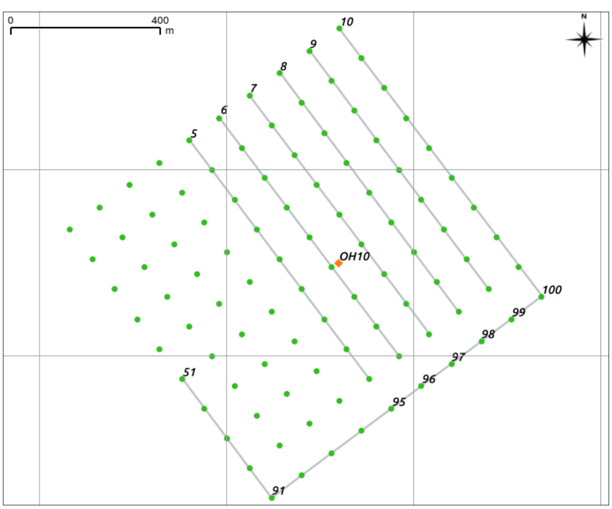

Figure 4: Grid designed to carry out GPR measurements in the area around the drill site of OH-10. Green dots denote marks of 100 m span between them. Grey lines show the sections that were covered by the GPR measurements. Continuous grey lines indicate the completed profiles. Other proposed lines were not possible to be completed due to adverse meteorological conditions.

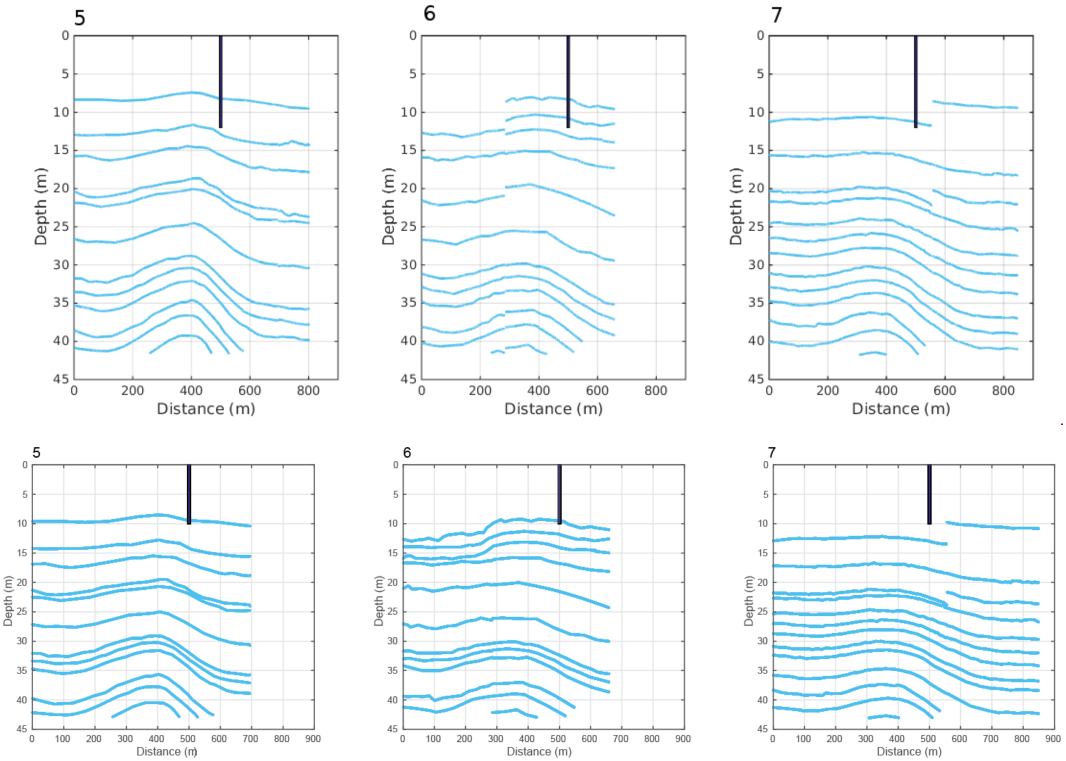

Figure 5: Layer interpretation (light blue lines) of radar imaging collected near the extracted the drill site of firn core OH-10. From left to right: 5, 6 and 7 mark the starting point of the measurement (see Fig. 4 for location). The black bars indicate the depth of the firn core retrieved (OH-10).

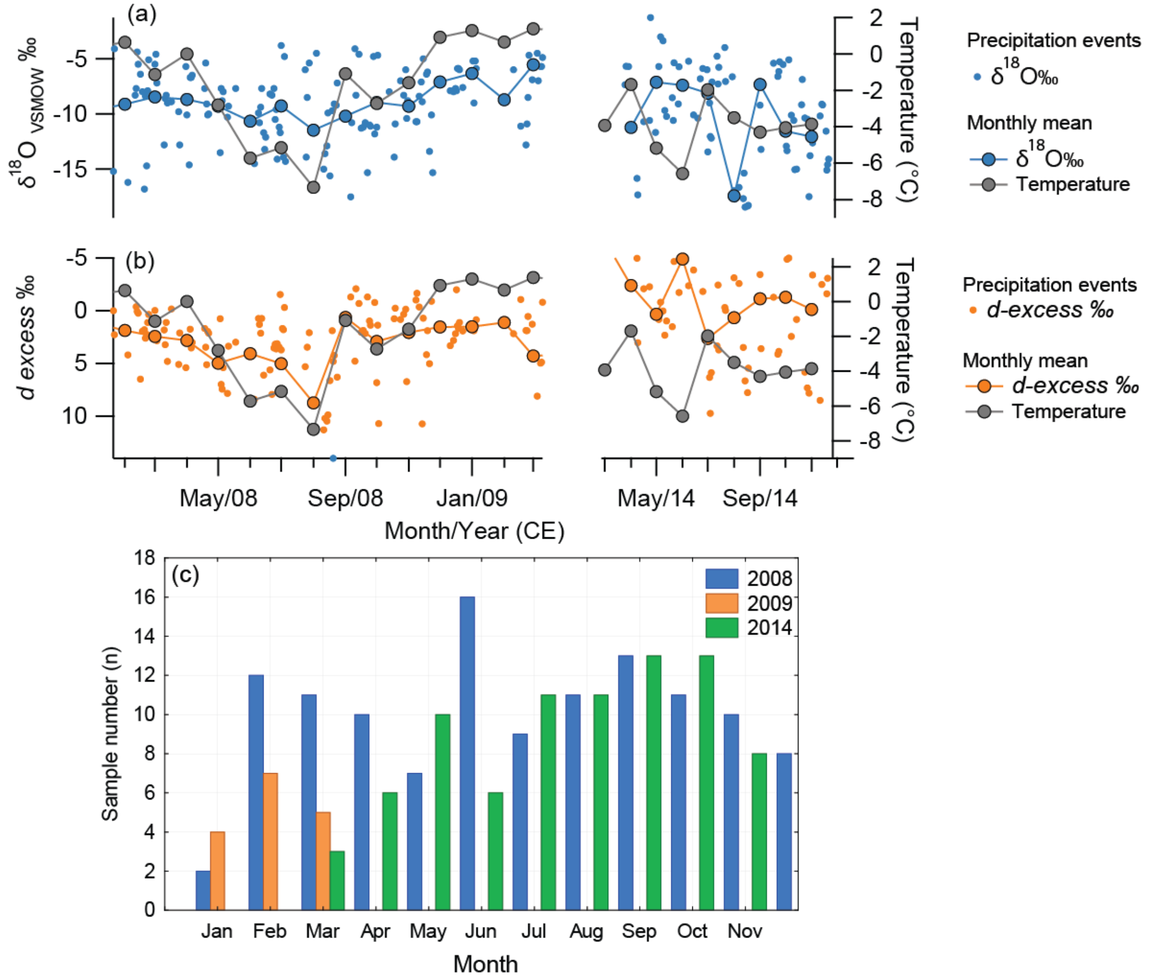

Figure 6~~7~~: Stable water isotope composition of precipitation events and air temperature at O'Higgins Station. (a) shows the $\delta^{18}O$ composition of precipitation of single daily events (small solid blue dots) and monthly means (big solid blue dots and line) and (b) deuterium excess (d_{excess}) of single daily events (small orange dots) and monthly means (big orange dots and line). In both (a) and (b) monthly mean air temperature is also shown (grey solid dots and line). (c) Histogram showing the monthly distribution of precipitation samples (n) collected at O'Higgins Station in 2008, 2009 and 2014

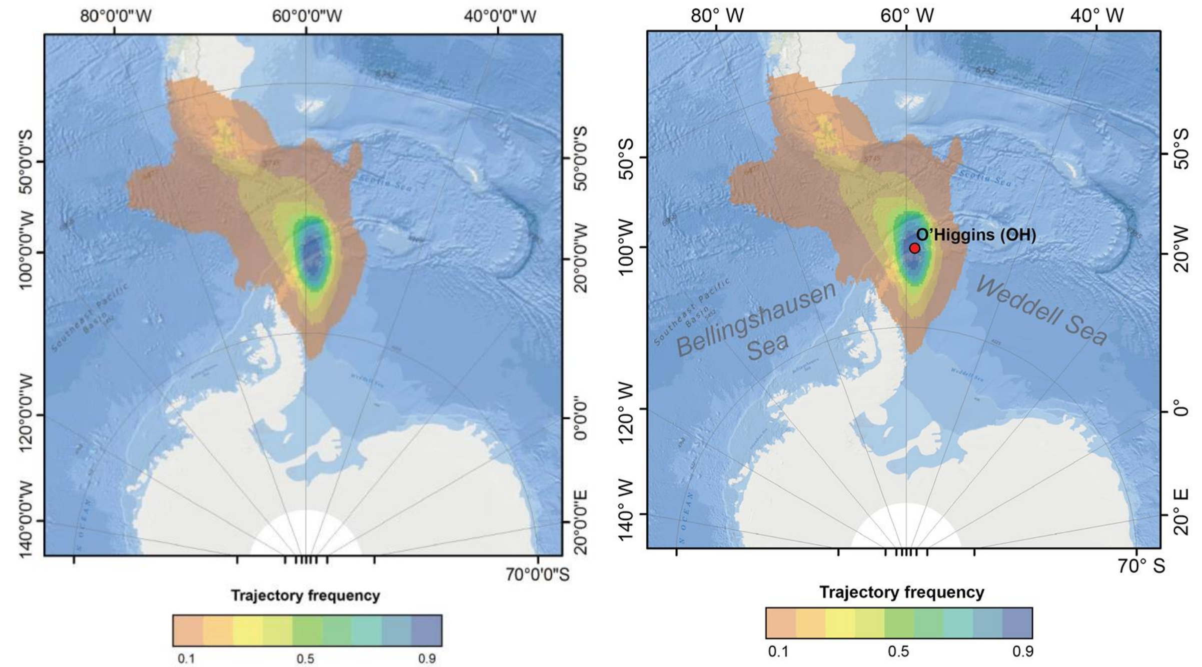

Figure 7~~6~~: Frequency distribution map of the main transport paths of air masses approaching the northern Antarctic Peninsula (AP~~I~~). Translucent red colours represent the lowest frequency and blue colours the higher frequency. In general most of the air masses arriving at the AP~~I~~ are coming from the Bellingshausen Sea and the South Pacif Ocean.

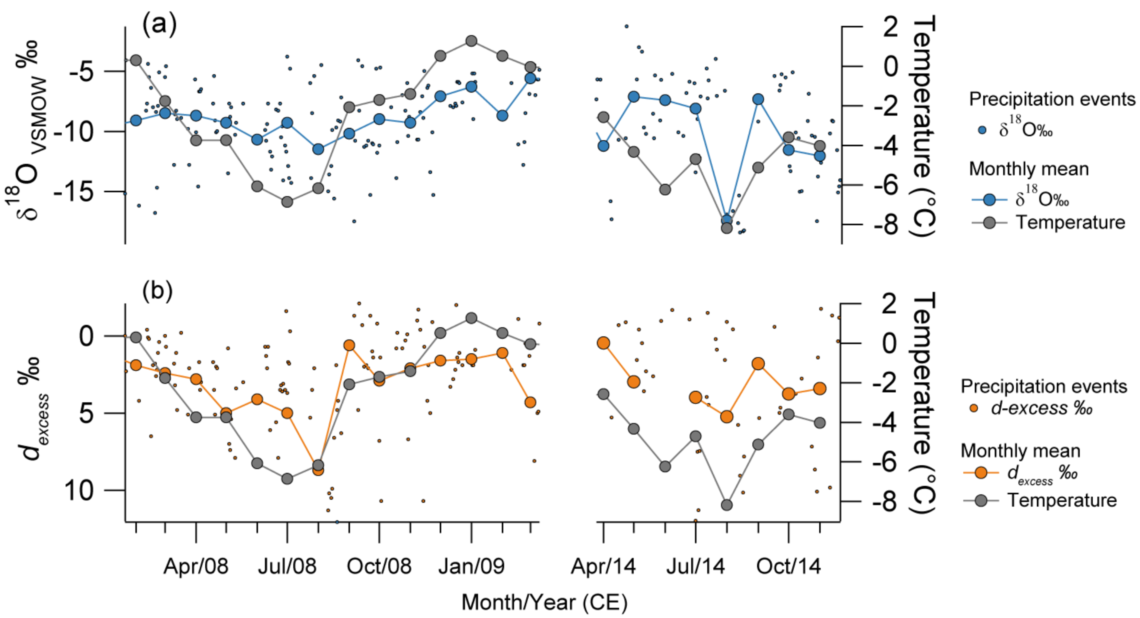

~~**Figure 7:** Stable water isotope composition of precipitation events and air temperature at O'Higgins Station. (a) shows the $\delta^{18}O$ composition of precipitation of single daily events (small solid blue dots) and monthly means (big solid blue dots and line) and (b) deuterium excess (d_{excess}) of single daily events (small orange dots) and monthly means (big orange dots and line). In both (a) and (b) monthly mean air temperature is also shown (grey solid dots and line).~~

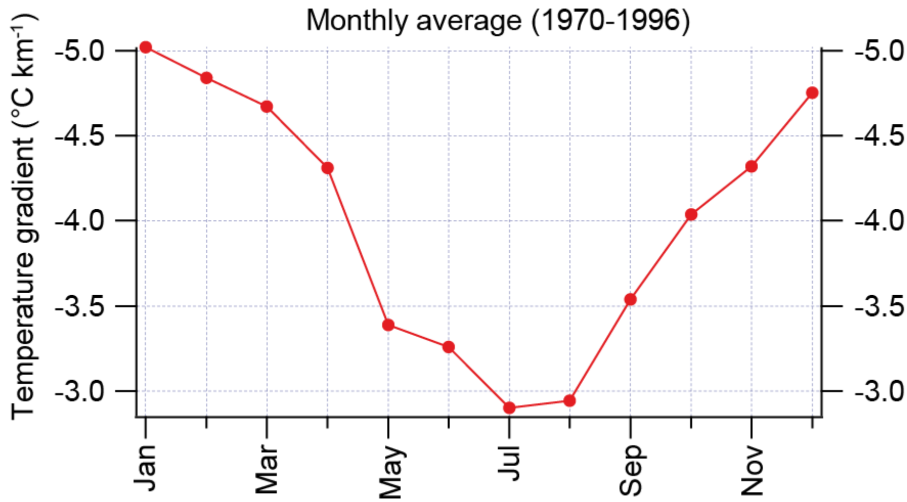

Figure 8: Temperature lapse rate from sea level to 850 hPa level at Bellingshausen station (BE), King George Island, Antarctica. The data is shown as the monthly mean value of observation between 1979 and 1996 (SCAR Reference Antarctic Data for Environmental Research).

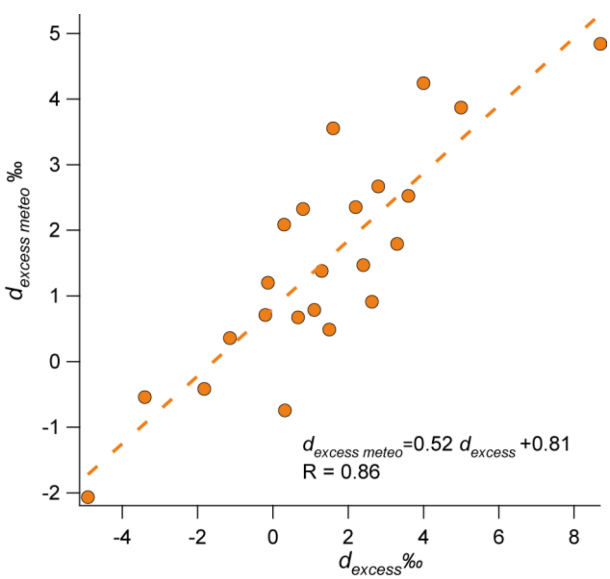

Figure 98: Correlation between monthly mean deuterium excess values (d_{excess}) from precipitation samples~~firn cores~~ and theoretical deuterium excess values calculated from meteorological parameters of the moisture source region ($d_{excess\ meteo}$) according to Uemura et al. (2008).

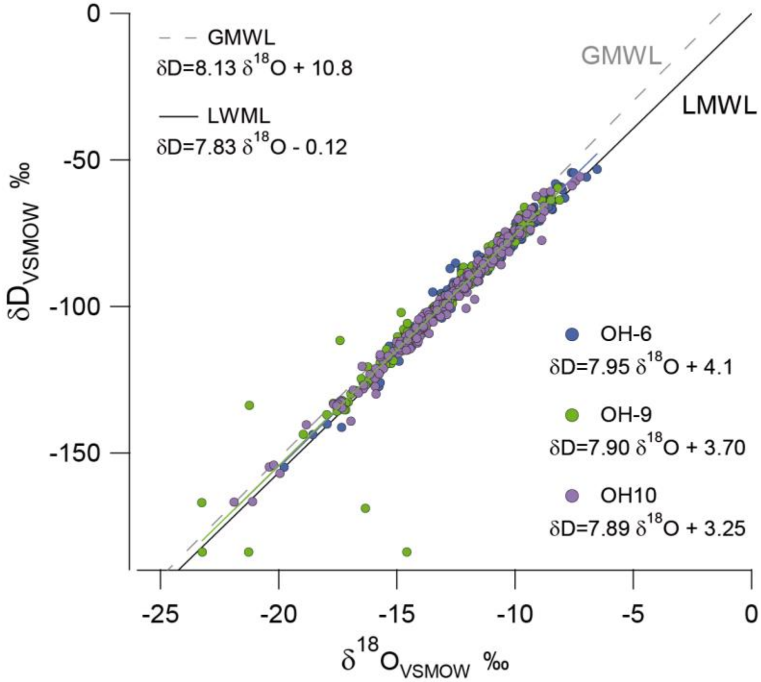

Figure 10~~9~~: Co-isotopic relationship of firn cores OH-6 (solid blue dots), OH-9 (solid green dots) and OH-10 (solid purple dots). All slopes and intercepts are very close to each other as well as to the global and local meteoric water line (GMWL – grey dashed line, and LMWL – black solid line, respecitvely). Stable water isotope analysis for each firn core was made at 5cm resolution, representing 630 samples in total.

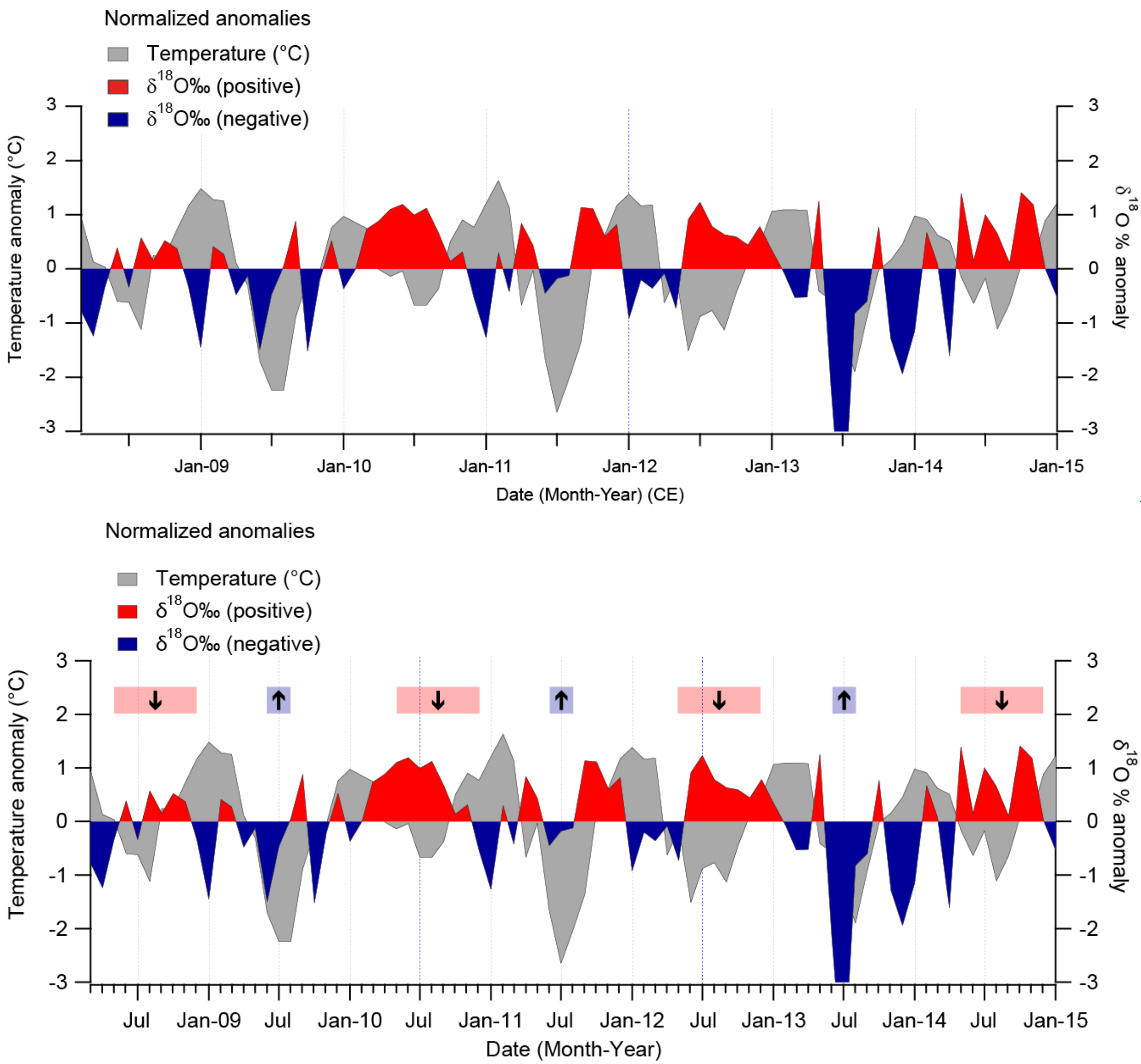

Figure 11~~10~~: Standarized anomalies for air (monthly mean) temperatures (solid grey colours) registered at Bellingshausen Station (BE) on King George Island and a composite $\delta^{18}O$ time series derived from firn cores OH-6, OH-9 and OH-10 from Laclavere Plateau (LCL). Upper translucid red (blue) boxes show period of positive (negative) anomalies, down (up) arrow shows the inverse (positive) stable water isoto – temperature relationship Both time series were detrended prior to constructing the time series of anomalies.

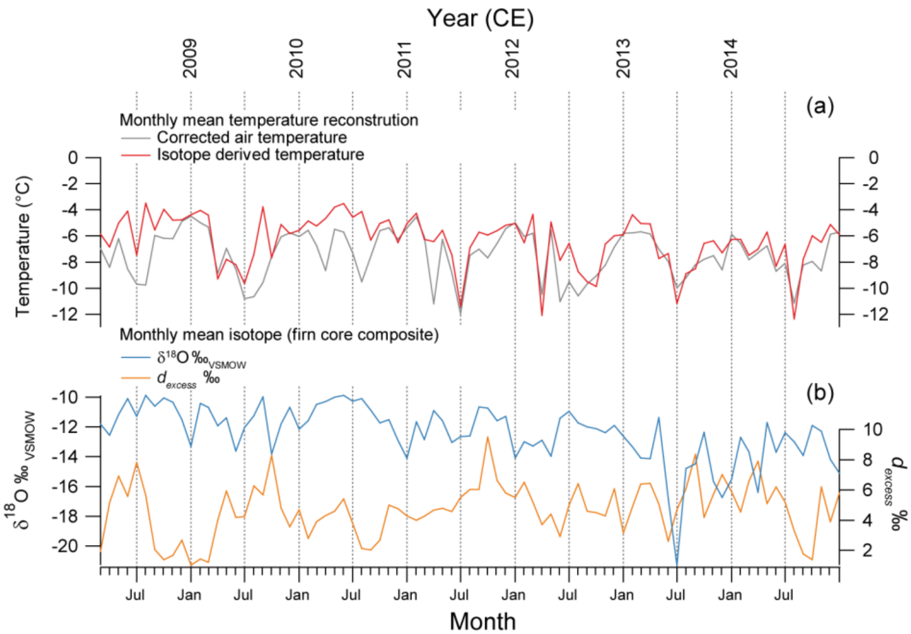

Figure 12~~11~~: (a) Monthly mean air temperature reconstruction for LCL between March 2008 and January 2015 based on air temperature corrected by a seasonal factor and altitudinal gradient (grey line) and based on a $\delta^{18}O$ composite time series derived from firn cores from LCL corrected by a seasonal factor (red line), respectively. (b) $\delta^{18}O$ and d_{excess} monthly mean composite time series of LCL firn cores used for the temperature reconstruction of the upper panel.

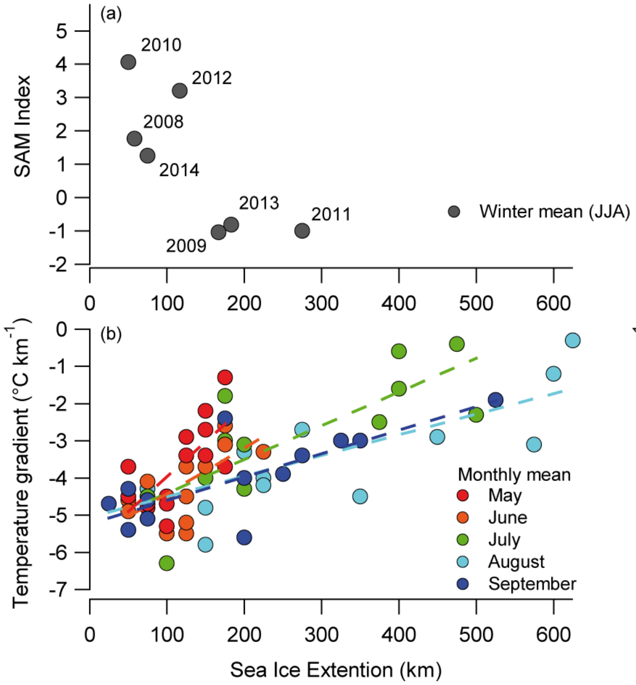

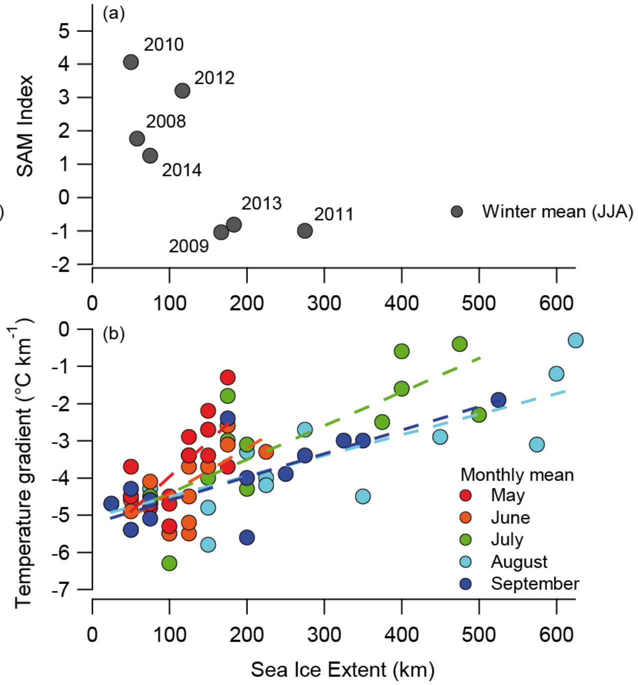

Figure 13~~12~~: Sea ice extent (SIE) from O'Higgins Station (OH) and its relationship to (a) the Southern Annular Mode and (b) to the temperature gradient between sea level and 1100 m a.s.l. at the Laclavere Plateau (LCL). SIE data is from the National Snow & Ice Data Center data set (NSIDC) ~~Hadley Centre Sea Ice and Sea Surface Temperature data set (HadISST)~~. Sea ice extent, defined as the extention of the sea region covered for at least 15% of ice ~~(Rayner et al., 2003b)~~, exhibits a negative relationship to the Southern Annular Mode between 2008 and 2014. The relationship to the temperature gradient is positive. A decreasing seasonal pattern of the temperature gradient can be observed from May to September (1979 – 1996).

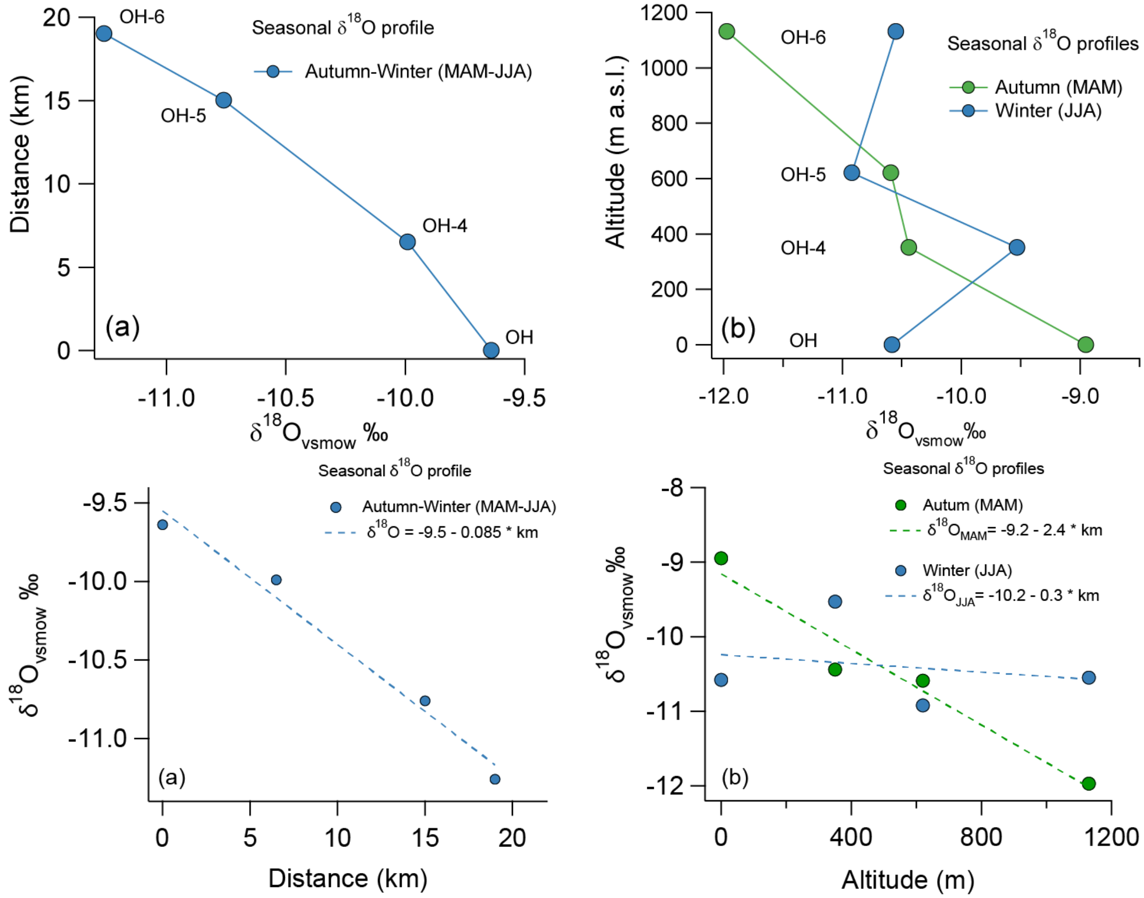

Figure <u>14</u>~~13~~: $\delta^{18}O$ profile with relation to (a) the distance from the coast at O'Higgins Station (OH) and at different points on the west flank of the AP~~I~~ (6.5 km (OH-4), 15 km (OH-5) and 19 km (OH-6)) and (b) altitude at 350 m (OH-4), 620 m (OH-5) and 1130 m a.s.l. (OH-6) during autumn (MAM) (green solid dots) and winter (JJA) (blue solid dots).

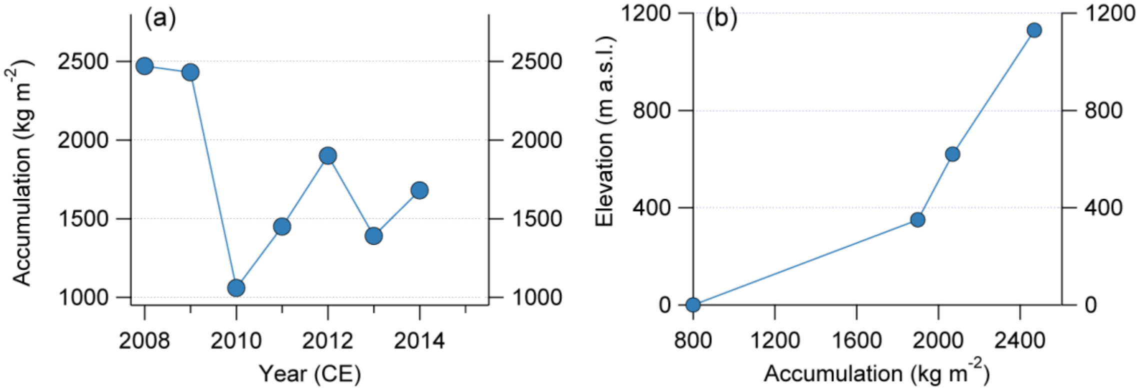

Figure 15~~14~~: (a) Accumulation rates for Plateau Laclavere during 2008 – 2014 estimated from the stable water isotope composition of firn cores OH-6, OH-9 and OH-10 and their respective density profiles. (b) Accumulation variability for the west flank of the northern Antarctic Peninsula from the coast to Laclavere Plateau. Accumulation rates were derived from precipitation at O'Higgins Station at sea level and firn cores (OH-4, OH-5 and OH-6) for higher altitudes.

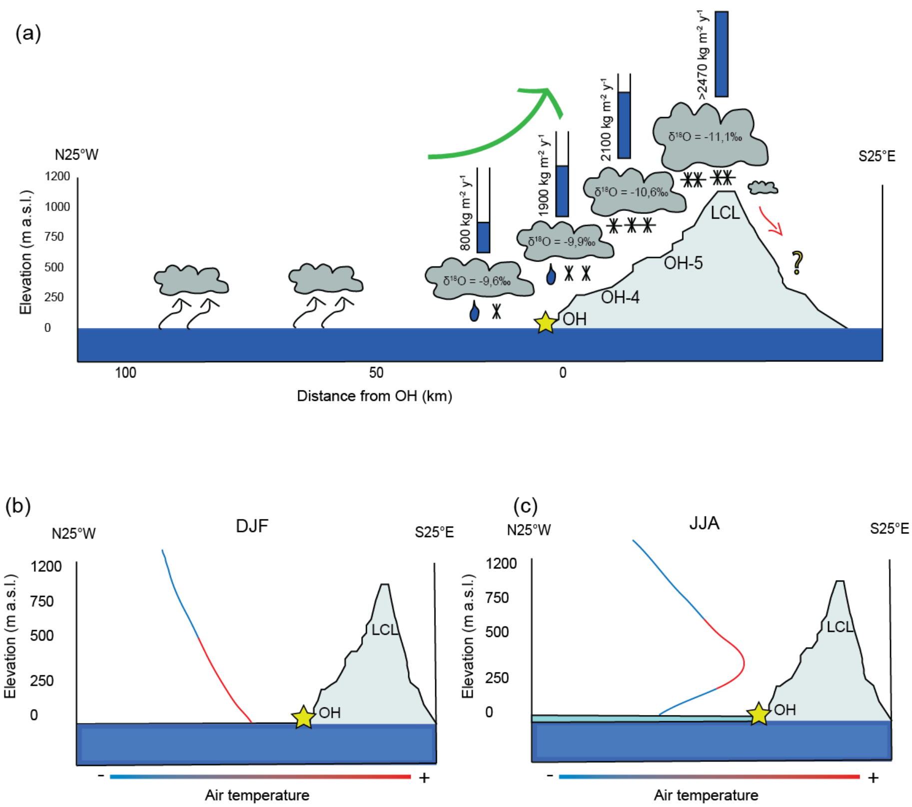

Figure 16~~15~~: (a) Schematic chart showing the orographic barrier effect of the AP~~I~~ on the stable water isotope depletion and accumulation rate at different altitudes, firn core locations (OH-4, OH-5 and OH-6) and distances from the coast (OH); (b) temperature gradient (adiabatic cooling) during DJF (summer) and sea–ice–free conditions; (c) inversion layer in the lower troposhere during sea–ice–covered conditions in JJA (winter).

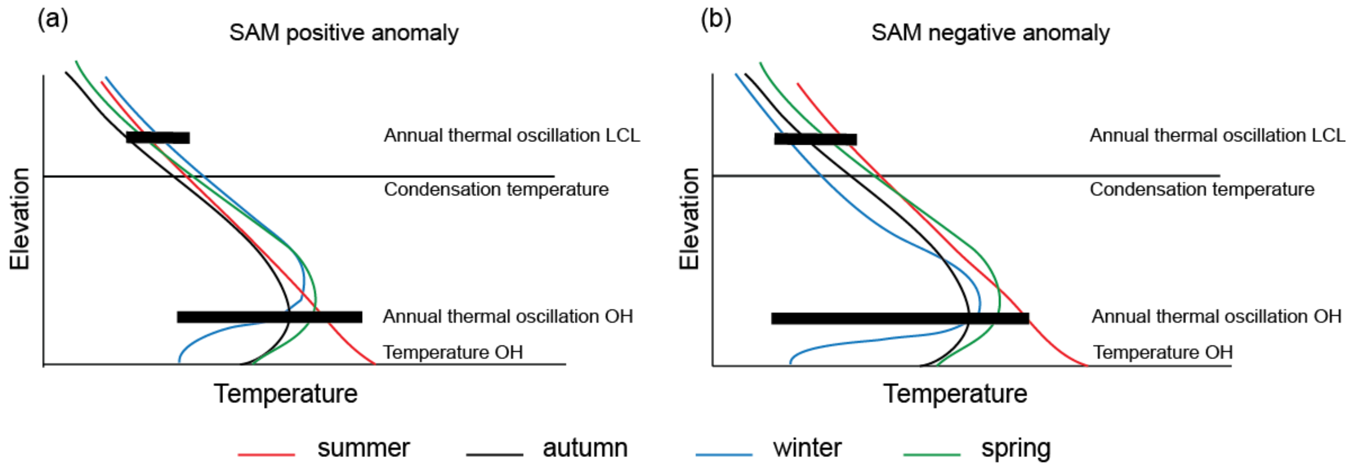

Figure ~~16~~17: Sea level to LCL temperature oscillation scheme during summer (DJF), autumn (MAM), winter (JJA) and spring under: (a) positive SAM anomaly conditions and (b) negative SAM anomaly conditions.

Table 1: Statistical summary of the geographical location and water stable isotope composition of all firn cores examined in this work. OH-4 and OH-5 correspond to cores retrieved on the west side of the AP~~I~~, whereas OH-6, OH-9 and OH-10 were retrieved at LCL on the east–west divide. All cores were analyzed in a 5 cm resolution.

Core	OH-4	OH-5	OH-6	OH-9	OH-10
Coordinates	57.80°W, 63.36°S	57.62°W, 63.38°S	57.76°W, 63.45°S	57.76°W, 63.45°S	57.76°W, 63.45°S
Altitude (m a.s.l.)	350	620	1130	1130	1130
Depth (m)	15.75	10.6	11.02	11.65	10.17
Drilling date	Jan 2009	Jan 2009	Jan 2010	Jan 2014	Jan 2015
$\delta^{18}O$ (‰)					
Mean	-10.4	-10.2	-12.0	-12.80	-12.94
Sdev	1.2	1.5	2.5	2.53	2.57
Min	-14.1	-14.2	-19.8	-23.25	-21.88
Max	-7.0	-7.2	-6.5	-8.12	-7.25
δD (‰)					
Mean	-78.9	-78.1	-91.4	-97.49	-98.81
Sdev	9.7	12.0	19.4	21.04	20.45
Min	-108.2	-111.2	-154.9	-183.80	-166.82
Max	-54.0	-52.1	-53.2	-59.62	-55.80
d_{excess} (‰)					
Mean	4.0	3.9	4.4	5.11	4.72
Sdev	1.5	1.7	2.8	1.90	2.66
Min	0.5	-0.6	-2.6	0.00	-6.50
Max	8.6	8.2	15.0	10.97	11.27
n (samples)	318	213	208	232	190

Table 2: Statistics of the stable water isotope composition of precipitation samples collected at OH Station on the AP~~I~~ 2008–2009 and 2014.

Station	O'Higgins	O'Higgins
Sampling interval	Feb 2008 – Mar 2009	Apr – Nov 2014
Coordinates	63.32°S, 57.90°W	63.32°S, 57.90°W
$\delta^{18}O$ (‰)		
Mean	-9.2	-10.12
Sdev	3.33	4.39
Min	-19.4	-18.43
Max	-3.8	-1.28
δD (‰)		
Mean	-70.5	-81.86
Sdev	26.44	34.21
Min	-150.6	-148.36
Max	-21.8	-15.99
d_{excess} (‰)		
Mean	2.7	3.84
Sdev	4.15	4.67
Min	-6.6	-1.75
Max	22.3	14.70
n (samples)	139	69

Table 3: Correlation between deuterium excess ($d_{excess\ meteo}$) values calculated from monthly mean meteorological data (SST and *rh*) and water stable isotope monthly means for all cores used in this study.

Core	OH-4	OH-5	OH-6	OH-9	OH-10
Time interval	Jan 2006 – Jan 2009	Mar 2007 – Jan 2009	Mar 2008 – Jan 2010	Feb 2010 – Jan 2014	Feb 2012 – Jan 2015
Corr. coefficient	0.72	0.79	0.81	0.78	0.67
p-value	<0.01	<0.01	<0.01	<0.01	<0.01

Table 4: Accumulation rates calculated for all firn cores used in this study. All rates are shown as seasonal and annual mean values with respect to the time interval covered by each core.

AP~~I~~ Accumulation (kg m^{-2})					
	Western Flank		LCL		
	OH-4	OH-5	OH-6	OH-9	OH-10
DJF-MAM	1121				
JJA-SON	1300				
2006	**2510**				
DJF-MAM	1650	>1380			
JJA-SON	1300	1150			
2007	**2950**	**>2530**			
DJF-MAM	1130	1020	>1530		
JJA-SON	770	1050	940		
2008	**1900**	**2070**	**>2470**		
DJF-MAM			1090		
JJA-SON			1340		
2009			**2430**		
DJF-MAM				700	
JJA-SON				360	
2010				**1060**	
DJF-MAM				680	
JJA-SON				770	
2011				**1450**	
DJF-MAM				1170	1080
JJA-SON				730	690
2012				**1900**	**1770**
DJF-MAM				890	930
JJA-SON				500	690
2013				**1390**	**1620**
DJF-MAM					630
JJA-SON					1050
2014					**1680**